

A Theoretical Framework for Electromechanically Reinforced Brillouin Scattering in Integrated Photonics Waveguides

Ali Dorostkar

¹ *Fractal Group, Isfahan, Iran**

Sayyed Reza Mirnaziry

² *Electrical Engineering Department, University of Qom, Qom, Iran*

Current theoretical demonstration of the Stimulated Brillouin scattering in waveguides composed of centrosymmetric materials is not applicable to describe the phenomenon in waveguides constituting non-centrosymmetric materials. The SBS in the latter problem, entails mutual coupling of the electric and acoustic waves due to piezoelectricity, and ends up to a different power conversion equation than that in a centrosymmetric material. In this study, we theoretically investigate Brillouin scattering in chip-scale waveguides with non-centrosymmetric material when excited by an Inter-Digital-Transducer. We explain how Brillouin scattering formulated in presence of externally injected acoustic waves, we demonstrate the effect of this external signal reinforcing Stimulated Brillouin scattering. We use the derived power conversion equations to study stimulated Brillouin scattering in a gallium arsenide nonowire. The Stokes amplification due to electromechanically reinforced SBS in this case study can grow several orders of magnitude higher than the values reported for a conventional SBS in a silicon nanowire; This enables reducing the waveguide length from centimeters to few hundred micrometers.

I. INTRODUCTION

Stimulated Brillouin Scattering (SBS) is a nonlinear process resulting from coherent interactions between photons and excited phonons in an optical propagation medium [1–5]. There have been prominent developments in the last decade to tailor Brillouin interactions in chip-scale platforms; To enhance the SBS nonlinearities, various configurations have been studied among them nonowires - either suspended or on substrate-, slot and rib waveguides and photonic crystal fibers have shown promising potential to increase the SBS gain [6–12] for the purpose of various functionalities such as in sensor, microwave photonics and lasing [4]. In harnessing SBS for integrated photonics the main challenge toward reaching higher values of SBS gain is to effectively confine both optic and acoustic waves simultaneously in a waveguide cross-section. This underlines the importance of both waveguide materials and geometry to enable co-propagation of optical and acoustic waves [13]. For instance, the optical modes in silicon nanowire on silica substrate is confined due to total internal reflection, however; due to the higher stiffness of silicon rather than SiO₂ there is a leaking of acoustic wave to the substrate. Chalcogenide glasses with relatively high refractive index and low stiffness, are also promising candidates to realize total internal reflection for both optical and acoustics waves [9]. Suspending the waveguide structures, despite the difficulty in their realization were also proposed to reach a mechanical isolation [8]. Despite these successes, enabling confinement of photon and phonon in silicon or popular semiconductor platform with

a feasible and robust manufacture still is challenging. As the Brillouin optomechanical coupling is restricted by optical and mechanical dissipations.

Recently, a great attention is drawn toward achieving Brillouin scattering in chip scale geometries using electromechanical excitation of phonon via interdigital transducers (IDT) [14–16]. Regarding this, the electromechanical Brillouin scattering (EBS) is a process wherein a radio frequency signal of generates acoustic waves, which is employed to contribute in power conversion of the injected optical pump [14]. It is shown that an acoustic wave at 16 GHz excited by IDT in an aluminum nitride (AlN) suspended waveguide scatters pump wave, which red-shifts it to the anti-Stokes sideband. However, there is a discrepancy between theoretical results and those obtained by experiment on demonstrating the relevant Brillouin interactions [14].

Current studies on SBS has also shown great interests on deploying acousto-optic platforms to harness piezo-optomechanical interactions; in [15] for instance, the acousto-optic modulation within silicon is demonstrated using IDT on the piezoelectric material AlN. Lithium niobate is another promising material for this platform addressed a high mechanical Q factor and an efficient piezoelectric transduction [17, 18]. In addition, several approaches are demonstrated to determine optimal condition for overlapping the electromechanically excited phonon with a phonon generated optomechanically in acousto-optic structures [19–21]. However, a general theoretical model is still needed to consider both EBS and SBS interactions in piezoelectric structures.

Here, we provide a detailed theoretical framework to study the effect of external piezoelectric forces induced by IDT on power conversion through the SBS in selected integrated photonic structures. We show how coupled mode equations for the SBS interactions are modified in

* m110alidorostkar@gmail.com

the presence of electromechanically injected phonons and how this forms a distinguished power conversion between pump and Stokes. To demonstrate what we call it Electromechanically Reinforced Stimulated Brillouin Scattering (ERSBS), we take the method presented in [7] and extend it to include the effect of piezoelectric forces. As we will show, piezoelectric force affects the SBS gain and leads to a modification on the whole coupled mode equations. Also, the strength of piezoelectric force that is a function of piezoelectric power, is a critical parameter in maximizing the Stokes amplification.

II. PRELIMINARIES AND DEFINITIONS

We begin by introducing the geometrical and parameters of the interacting waves in establishing the coupled mode equations. Figure 1 shows a schematic of a nanowire composed of a piezoelectric material of rectangular cross section with a width of W and height of H in the XY plane, capable of guiding light in at least one optical mode that is translationally invariant along the z -axis. As shown in the figure, an IDT is placed on the waveguide to induce acoustic waves. Assuming that pump and Stokes co-propagate along the externally induced acoustic wave, we call the process forward ERSBS. If instead pump and Stokes contra-propagate, while pump is in the direction of the external acoustic wave, a backward ERSBS occurs. The acoustic wave induced by IDT for forward or backward process has the same propagation direction with pump -or with the acoustic wave excited via pump-Stokes interactions. An optical mode propagating through the nanowire at frequency of ω_i with a propagation constant k_i ($i = p$ (pump) or s (Stokes)) can be expressed by

$$\mathbf{E}_i = A_i(z, t) \tilde{\mathbf{e}}_i(\mathbf{x}, \mathbf{y}) e^{i(k_i z - \omega_i t)} + c.c., \quad (1)$$

in which $A_i(z, t)$ is the envelope that varies slowly along the waveguide and $\tilde{\mathbf{e}}_i(\mathbf{x}, \mathbf{y})$ denotes the mode profile. Note that the term *c.c.* in Eq. (1) refers to complex conjugate components. Similarly, the acoustic displacement wave at frequency of Ω with a propagation constant q takes the following ansatz

$$\mathbf{U} = b(z, t) \tilde{\mathbf{u}}(\mathbf{x}, \mathbf{y}) e^{i(qz - \Omega t)} + c.c., \quad (2)$$

where $b(z, t)$ and $\tilde{\mathbf{u}}(\mathbf{x}, \mathbf{y})$ are the acoustic envelope and the mode profile, respectively.

III. COUPLED-MODE EQUATIONS IN THE PRESENCE OF CENTROSYMMETRIC MATERIALS

We first consider that the waveguide shown in Fig.1 is composed of a centrosymmetric materials such as silicon. Then, the coupled-mode equations between pump, Stokes and the acoustic envelopes are expressed by [7]

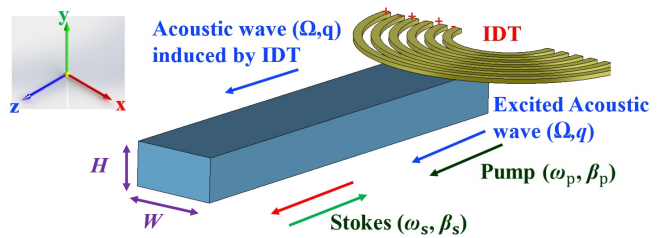


FIG. 1. Schematic of the ERSBS interactions in a waveguide aligned along the z -axis with a cross section of W (width) and H (height). Backward ERSBS (Stokes wave represented by the green arrow) and forward ERSBS (Stokes wave in red) where pump and acoustic waves are represented by black and blue arrows, respectively.

$$\frac{\partial A_p}{\partial z} = -\frac{i\omega_p}{\mathcal{P}_p} \tilde{Q}_p A_s b, \quad (3)$$

$$\frac{\partial A_s}{\partial z} = -\frac{i\omega_s}{\mathcal{P}_s} \tilde{Q}_s A_p b^*, \quad (4)$$

$$\frac{\partial b}{\partial z} + \alpha_{ac} b = \frac{-i\Omega}{\mathcal{P}_{ac}} \tilde{Q}_b A_p A_s^*, \quad (5)$$

where Q_i is an overlap integral, ω_i is the optical frequency of pump and Stokes, Ω is the acoustic frequency and \mathcal{P}_k ($k = p, s, ac$) is Poynting power for the optical and acoustic modes [7]. The coefficient of α_{ac} is the acoustic decay parameter. The overlap integral Q_i is defined as

$$\tilde{Q}_p^* = \tilde{Q}_s = \tilde{Q}_b = \int (\tilde{\mathbf{u}}^* \cdot \tilde{\mathbf{f}}_{EM}) ds, \quad (6)$$

where $(\tilde{\mathbf{f}}_{EM})$ denotes the optical forces [7].

IV. COUPLED-MODE EQUATIONS OF SBS IN A NON-CENTROSYMMETRIC MATERIAL

Now, we assume that the waveguide in Fig.1 is composed of a non-centrosymmetric material. We also limit our study to non-centrosymmetric materials with piezoelectric properties; this means that crystals with non-centrosymmetric cubic class 432 that do not possess piezoelectric properties are not considered here. The piezoelectricity can influence acoustic parameters of the excited modes in the waveguide. Provided that an IDT is fed by a radio frequency (RF) signal with an operating frequency equal to the interested acoustic mode, an extra phased-matched mechanical power is added to the one excited via SBS interactions. In the following, We first look at the relation between the piezoelectric signal and its resultant acoustic envelope, then use it to modify the coupled mode equations between pump and Stokes.

A. Wave interactions in the presence of an externally injected piezoelectric signal

We assume that the IDT generates an acoustic signal to a piezoelectric waveguide. We will add this piezoelectric signal to the wave equations because the acoustic mode must satisfy the required SBS phase matching condition. The induced mechanical vibrations in a piezoelectric waveguide leads an electromagnetic (EM) wave propagating along the waveguide at an identical frequency to the acoustic signal (i.e. in the RF range) and vice versa. The electrical displacement wave (\mathbf{D}_{RF}) corresponding to this wave is related to the mechanical strain by [22]

$$\mathbf{D}_{\text{RF}} = \boldsymbol{\epsilon} \cdot \mathbf{E}_{\text{RF}} + \mathbf{e} : \mathbf{S} + c.c., \quad (7)$$

where $\boldsymbol{\epsilon}$ is the permittivity, \mathbf{E}_{RF} is the electric wave, \mathbf{e} is the piezoelectric stress tensor and \mathbf{S} denotes strain produced by IDT and pump-Stokes interactions. In addition, the double dot indicates the product of a third rank tensor (i.e. the piezoelectric stress tensor) and a second rank tensor (i.e. the strain). It must to be mentioned that the extra term ($\mathbf{e} : \mathbf{S}$) comes from the material polarization. As strain is applied to the piezoelectric medium, this will change the orientation of dipole arrangements in the material and leads to a net dipole moment per unit volume [23]. In addition, another RF signal can be generated from the pump and Stokes interference through second order nonlinearity, however; as shown in the appendix A its contribution is small enough to be neglected. Now, the electromagnetic (EM) wave equation for a piezoelectric medium in the RF domain can be described as:

$$\begin{aligned} \nabla \times \nabla \times \mathbf{E}_{\text{RF}} &= -\mu_0 \frac{\partial^2 \mathbf{D}_{\text{RF}}}{\partial t^2} \\ &= -\mu_0 \left(\frac{\partial^2 (\boldsymbol{\epsilon} \cdot \mathbf{E}_{\text{RF}})}{\partial t^2} + \frac{\partial^2 (\mathbf{e} : \nabla \mathbf{U})}{\partial t^2} \right). \end{aligned} \quad (8)$$

We note that in Eq. (8), it is assumed that \mathbf{E}_{RF} is induced by the IDT and impact by optical interactions

through acoustic wave; in the presence of pump and Stokes signal, an extra phased matched RF signal is expected to be added to that generated by IDT.

Generally, the electric wave \mathbf{E}_{RF} can be separated into a rotational and an irrotational part; The irrotational wave is called a quasi-static wave and can be expressed as a gradient of an scalar potential (Φ_{RF}) [22]. Note that with neglecting the rotational wave by taking the divergence as shown in Eq. (11) the quasi-static model is an appropriate model for many piezoelectric problems [20].

$$\mathbf{E}_{\text{RF}} = \mathbf{E}_{\text{RF}}^{\text{rot.}} + \mathbf{E}_{\text{RF}}^{\text{irrot.}} = \mathbf{E}_{\text{RF}}^{\text{rot.}} - \nabla \Phi_{\text{RF}}. \quad (9)$$

The piezopotential (Φ_{RF}) is a time-varying scalar function, which varies along the waveguide with respect to \mathbf{E}_{RF} . The piezopotential can be expressed by

$$\Phi_{\text{RF}}(x, y, z, t) = \Psi(z, t) \phi(x, y) e^{i(qz - \Omega t)} + c.c. = \Psi \tilde{\phi} + c.c., \quad (10)$$

where Ψ is the potential envelope and $\tilde{\phi}_{\text{RF}}$ is the potential scalar mode. By taking the divergence over Eq. (8), we have:

$$\begin{aligned} \nabla \cdot \left(\nabla \times \nabla \times \mathbf{E}_{\text{RF}} \right) &= \nabla \cdot \left(-\mu_0 \frac{\partial^2 \mathbf{D}_{\text{RF}}}{\partial t^2} \right) \\ &= \nabla \cdot \left(-\mu_0 \frac{\partial^2 (\boldsymbol{\epsilon} \cdot \mathbf{E}_{\text{RF}})}{\partial t^2} - \mu_0 \frac{\partial^2 (\mathbf{e} : \nabla \mathbf{U})}{\partial t^2} \right) = 0, \end{aligned} \quad (11)$$

where $\nabla \cdot (\boldsymbol{\epsilon} \cdot \mathbf{E}_{\text{RF}}^{\text{rot.}}) = 0$ and $\mathbf{E}_{\text{RF}}^{\text{irrot.}} = -\nabla \Phi_{\text{RF}}$. After simplifying Eq. (11), we have

$$\nabla \cdot \left(-\boldsymbol{\epsilon} \cdot \nabla (\Psi \tilde{\phi}) + \mathbf{e} : \nabla (b \tilde{\mathbf{u}}) \right) = 0. \quad (12)$$

Now, by projecting $\tilde{\phi}^* \times (-i\Omega)$ on Eq. (12) and assuming small signal approximation together with neglecting higher order derivatives of Ψ we have

$$\begin{aligned} < (i\Omega \tilde{\phi}) | -\nabla \cdot (\boldsymbol{\epsilon} \cdot \nabla (\Psi \tilde{\phi})) + \nabla \cdot (\mathbf{e} : \nabla (b \tilde{\mathbf{u}})) > \approx < (i\Omega \tilde{\phi}) | -\frac{\partial \Psi}{\partial z} (([\hat{a}_z]_{1 \times 3} \cdot (\boldsymbol{\epsilon} \cdot \nabla \tilde{\phi}) + \nabla \cdot (\boldsymbol{\epsilon} \cdot [\tilde{\phi}]_z)) \\ &- \Psi (\nabla \cdot (\boldsymbol{\epsilon} \cdot \nabla \tilde{\phi})) + \frac{\partial b}{\partial z} (([\hat{a}_z]_{1 \times 3} \cdot (\mathbf{e} : \nabla \tilde{\mathbf{u}})) + \nabla \cdot (\mathbf{e} : [\tilde{\mathbf{u}}])) + b (\nabla \cdot (r : \nabla \tilde{\mathbf{u}})) > = 0, \end{aligned} \quad (13)$$

where $[\hat{a}_z]_{1 \times 3}$ is the unit vector $[0, 0, 1]$, $[\tilde{\phi}]_z$ is defined as $[0, 0, \tilde{\phi}]$ and $[\tilde{\mathbf{u}}]$ denotes $[0, 0, \tilde{\mathbf{u}}_z, \tilde{\mathbf{u}}_y, \tilde{\mathbf{u}}_x, 0]^T$. Thus, the relation between the piezopotential envelope and its corresponding acoustic envelope takes the following form

$$\frac{\partial \Psi}{\partial z} M_{\text{RF}}^{(1)} + \Psi M_{\text{RF}}^{(2)} = \frac{\partial b}{\partial z} M_{\text{RF}}^{(3)} + b M_{\text{RF}}^{(4)}, \quad (14)$$

where the coefficient $M_{\text{RF}}^{(i)}$ ($i = 1, 2, 3, 4$) is an integral expressed by:

$$\begin{aligned}
M_{\text{RF}}^{(1)} &= (-i\Omega) \int \tilde{\phi}^* \left(([\hat{a}_z]_{1 \times 3} \cdot (\boldsymbol{\epsilon} \cdot \nabla \tilde{\phi})) + \nabla \cdot (\boldsymbol{\epsilon} \cdot [\tilde{\phi}]_z) \right) ds, \\
M_{\text{RF}}^{(2)} &= (-i\Omega) \int \tilde{\phi}^* (\nabla \cdot (\boldsymbol{\epsilon} \cdot \nabla \tilde{\phi})) ds, \\
M_{\text{RF}}^{(3)} &= (-i\Omega) \int \tilde{\phi}^* \left(([\hat{a}_z]_{1 \times 3} \cdot (\mathbf{e} : \nabla \tilde{\mathbf{u}})) + \nabla \cdot (\mathbf{e} : [\tilde{\mathbf{u}}]) \right) ds, \\
M_{\text{RF}}^{(4)} &= (-i\Omega) \int \tilde{\phi}^* (\nabla \cdot (\mathbf{e} : \nabla \tilde{\mathbf{u}})) ds.
\end{aligned} \tag{15}$$

By making an extra z-derivative of the piezopotential envelope of Eq. (14) and neglecting the second order derivatives of b and Ψ , we have

$$\frac{\partial \Psi}{\partial z} M_{\text{RF}}^{(2)} \approx \frac{\partial b}{\partial z} M_{\text{RF}}^{(4)}, \tag{16}$$

Now, the piezopotential envelope (Ψ) can be obtained by substituting Eq. (16) in Eq. (14)

$$\Psi \approx \frac{\partial b}{\partial z} \left(\frac{M_{\text{RF}}^{(3)} - \frac{M_{\text{RF}}^{(1)} M_{\text{RF}}^{(4)}}{M_{\text{RF}}^{(2)}}}{M_{\text{RF}}^{(2)}} \right) + b \frac{M_{\text{RF}}^{(4)}}{M_{\text{RF}}^{(2)}}. \tag{17}$$

$$\begin{aligned}
\mathbf{F}_{\text{piezo}} &= \nabla \cdot \mathbf{T}_{\text{piezo}} = -\nabla \cdot (\mathbf{e} \cdot \mathbf{E}_{\text{RF}}) = \nabla \cdot (\mathbf{e} \cdot \nabla (\Psi \tilde{\phi})) + c.c., \\
&\approx \frac{\partial \Psi}{\partial z} \left(([\hat{a}_z]_{3 \times 6} \cdot (\mathbf{e} \cdot \nabla \tilde{\phi})) + \nabla \cdot (\mathbf{e} \cdot [\tilde{\phi}]_z) \right) + \Psi \left(\nabla \cdot (\mathbf{e} \cdot \nabla \tilde{\phi}) \right) + c.c. = \frac{\partial \Psi}{\partial z} \tilde{\mathbf{f}}_{1,\text{piezo}} + \Psi \tilde{\mathbf{f}}_{2,\text{piezo}} + c.c.,
\end{aligned} \tag{20}$$

where $\tilde{\mathbf{f}}_{1,\text{piezo}}$ and $\tilde{\mathbf{f}}_{2,\text{piezo}}$ are piezoelectric forces and the matrix $[\hat{a}_z]_{3 \times 6}$ is

$$[\hat{a}_z]_{3 \times 6} = \begin{bmatrix} 0 & 0 & 0 & 0 & 1 & 0 \\ 0 & 0 & 0 & 1 & 0 & 0 \\ 0 & 0 & 1 & 0 & 0 & 0 \end{bmatrix}. \tag{21}$$

$$\begin{aligned}
\tilde{Q}_{1,\text{piezo}} &= \int \tilde{\mathbf{u}}^* \cdot \left(([\hat{a}_z]_{3 \times 6} \cdot (\mathbf{e} \cdot \nabla \tilde{\phi})) + \nabla \cdot (\mathbf{e} \cdot [\tilde{\phi}]_z) \right) ds = \int (\tilde{\mathbf{u}}^* \cdot \tilde{\mathbf{f}}_{1,\text{piezo}}) ds, \\
\tilde{Q}_{2,\text{piezo}} &= \int \tilde{\mathbf{u}}^* \cdot (\nabla \cdot (\mathbf{e} \cdot \nabla \tilde{\phi})) ds = \int (\tilde{\mathbf{u}}^* \cdot \tilde{\mathbf{f}}_{2,\text{piezo}}) ds.
\end{aligned} \tag{22}$$

The optical force \mathbf{F}_{EM} is predominantly originated from the electrostrictive (ES) force and the radiation pressure (RP) [6]

$$\mathbf{F}_{\text{EM}} = \mathbf{F}_{\text{ES}} + \mathbf{F}_{\text{RP}}, \tag{23}$$

and an appropriate ansatz for \mathbf{F}_{EM} with an optical force

B. Acoustic wave in a piezoelectric Material

We here derive an envelope acoustic differential equation from the acoustic wave equation for a non-centrosymmetric medium in the presence of piezoelectric and optical forces. The acoustic wave equation is expressed by [22]

$$\nabla \cdot \mathbf{T} + \mathbf{F}_{\text{Piezo}} + \mathbf{F}_{\text{EM}} = \rho \partial_t^2 \mathbf{U}, \tag{18}$$

where \mathbf{T} , $\mathbf{F}_{\text{piezo}}$ and \mathbf{F}_{EM} are normal stress, piezoelectric force and the optically induced optical force, respectively. The total stress (\mathbf{T}_{tot}) in piezoelectric material is divided to two parts of stress (\mathbf{T}) and piezoelectric stress ($\mathbf{T}_{\text{piezo}}$) and takes the following form [22]

$$\begin{aligned}
\mathbf{T}_{\text{tot}} &= \mathbf{T} + \mathbf{T}_{\text{piezo}} = \mathbf{c} : \mathbf{S} + \boldsymbol{\eta} : \frac{\partial \mathbf{S}}{\partial t} - \mathbf{e} \cdot \mathbf{E}_{\text{RF}}, \\
\mathbf{T} &= \mathbf{c} : \mathbf{S} + \boldsymbol{\eta} : \frac{\partial \mathbf{S}}{\partial t}, \\
\mathbf{T}_{\text{piezo}} &= -\mathbf{e} \cdot \mathbf{E}_{\text{RF}},
\end{aligned} \tag{19}$$

where \mathbf{c} and $\boldsymbol{\eta}$ are stiffness and viscosity tensors, respectively. The stress in a non-centrosymmetric material has an extra term in comparison to a centrosymmetric material. This term emerges as a piezoelectric force in the coupled mode equation

The piezoelectric overlap integral can be expressed by projecting the piezoelectric forces on the excited acoustic mode.

mode $\tilde{\mathbf{f}}_{\text{EM}}$ is [7]

$$\mathbf{F}_{\text{EM}} = A_p A_s^* \tilde{\mathbf{f}}_{\text{EM}} e^{-i\Omega t} + c.c., \tag{24}$$

By applying Eq. (2) and Eq. (19) in the acoustic wave equation and dropping higher order terms in the steady state regime we have

$$\begin{aligned} & \frac{\partial b}{\partial z} \left[\left([\hat{a}_z]_{3 \times 6} \cdot (\mathbf{c} : \nabla \tilde{\mathbf{u}}) + \nabla \cdot (\mathbf{c} : [\tilde{\mathbf{u}}]) \right) + \left((-i\Omega) \left(([\hat{a}_z]_{3 \times 6} \cdot (\boldsymbol{\eta} : \nabla \tilde{\mathbf{u}})) + \nabla \cdot (\boldsymbol{\eta} : [\tilde{\mathbf{u}}]) \right) \right) \right] \\ & + b \left[\nabla \cdot (\mathbf{c} : \nabla \tilde{\mathbf{u}}) + ((-i\Omega)(\nabla \cdot (\boldsymbol{\eta} : \nabla \tilde{\mathbf{u}})) + (\rho\Omega^2 \tilde{\mathbf{u}})) \right] + \frac{\partial \Psi}{\partial z} \tilde{\mathbf{f}}_{1,\text{piezo}} + \Psi \tilde{\mathbf{f}}_{2,\text{piezo}} + A_p A_s^* \tilde{\mathbf{f}}_{\text{EM}} + c.c. = 0. \end{aligned} \quad (25)$$

We now project the acoustic velocity mode $\tilde{\mathbf{v}}^*$ on Eq. (25)

$$\begin{aligned} & \langle \tilde{\mathbf{v}} | \frac{\partial b}{\partial z} \left[\left([\hat{a}_z]_{3 \times 6} \cdot (\mathbf{c} : \nabla \tilde{\mathbf{u}}) + \nabla \cdot (\mathbf{c} : [\tilde{\mathbf{u}}]) \right) + \left((-i\Omega) \left(([\hat{a}_z]_{3 \times 6} \cdot (\boldsymbol{\eta} : \nabla \tilde{\mathbf{u}})) + \nabla \cdot (\boldsymbol{\eta} : [\tilde{\mathbf{u}}]) \right) \right) \right] \right. \\ & \left. + b \left[\nabla \cdot (\mathbf{c} : \nabla \tilde{\mathbf{u}}) + ((-i\Omega)(\nabla \cdot (\boldsymbol{\eta} : \nabla \tilde{\mathbf{u}})) + (\rho\Omega^2 \tilde{\mathbf{u}})) \right] + \frac{\partial \Psi}{\partial z} \tilde{\mathbf{f}}_{1,\text{piezo}} + \Psi \tilde{\mathbf{f}}_{2,\text{piezo}} + A_p A_s^* \tilde{\mathbf{f}}_{\text{EM}} + c.c. \right\rangle = 0. \end{aligned} \quad (26)$$

Then, by knowing that the eigenmode $\tilde{\mathbf{u}}$ (i.e. $b = 1$)

satisfies [7]

$$\nabla \cdot (\mathbf{c} : \nabla \tilde{\mathbf{u}}) + (\rho\Omega^2 \tilde{\mathbf{u}}) = 0, \quad (27)$$

the differential equation governing the variations of the acoustic envelope is given by

$$\frac{\partial b}{\partial z} + \alpha_{\text{ac}} b = \frac{-i\Omega \tilde{Q}_b}{\mathcal{P}_{\text{ac}} + i\mathcal{P}_{\text{LOSS}}} A_p A_s^* + \frac{-i\Omega \tilde{Q}_{1,\text{piezo}}}{\mathcal{P}_{\text{ac}} + i\mathcal{P}_{\text{LOSS}}} \frac{\partial \Psi}{\partial z} + \frac{-i\Omega \tilde{Q}_{2,\text{piezo}}}{\mathcal{P}_{\text{ac}} + i\mathcal{P}_{\text{LOSS}}} \Psi, \quad (28)$$

where α_{ac} , \mathcal{P}_{ac} , $\mathcal{P}_{\text{LOSS}}$, $\tilde{Q}_{i,\text{piezo}}$ ($i=1,2$) and \tilde{Q}_b are the linear loss coefficient, acoustic Poynting power, acoustic loss power and overlap integrals of piezoelectric and opto-acoustic, respectively. The acoustic loss coefficient α_{ac} is obtained by

$$\alpha_{\text{ac}} = \frac{\Omega^2}{(\mathcal{P}_{\text{ac}} + i\mathcal{P}_{\text{LOSS}})} \int \tilde{\mathbf{u}}^* \cdot ((\nabla \cdot (\boldsymbol{\eta} : \nabla \tilde{\mathbf{u}})) ds, \quad (29)$$

and acoustic loss power is

$$\begin{aligned} \mathcal{P}_{\text{LOSS}} = \Omega \int \tilde{\mathbf{u}}^* \cdot \left((-i\Omega) \left(([\hat{a}_z]_{3 \times 6} \cdot (\boldsymbol{\eta} : \nabla \tilde{\mathbf{u}})) \right. \right. \\ \left. \left. + \nabla \cdot (\boldsymbol{\eta} : \tilde{\mathbf{u}}) \right) \right) ds. \end{aligned} \quad (30)$$

The first part of $\frac{\partial b}{\partial z}$ coefficient in Eq. (26) can be denoted by the use of approximation applied in [7] equalized to acoustic Poynting power (\mathcal{P}_{ac}) as shown in Eq. (69) ($\mathcal{P}_{\text{M}}^{\text{pure}}$).

$$\mathcal{P}_{\text{ac}} \approx i\Omega \int \tilde{\mathbf{u}}^* \cdot \left([\hat{a}_z]_{3 \times 6} \cdot (\mathbf{c} : \nabla \tilde{\mathbf{u}}) + \nabla \cdot (\mathbf{c} : \tilde{\mathbf{u}}) \right) ds. \quad (31)$$

C. Optical Waves in a Non-centrosymmetric Material

In a waveguide in the present of both pump and Stokes, the total electric field can be expressed as a superposition of pump and stokes waves

$$\mathbf{E} = \mathbf{E}_p + \mathbf{E}_s. \quad (32)$$

In a perturbed waveguide, each field component component e.g. \mathbf{E}_p has two parts; a non-perturbed and a perturbed term due to the interaction with acoustic and Stokes waves [7]. The latter, leads to temporal change in the refractive index. However, this is not the only source of change in refractive index of a piezoelectric material, as here the electrooptic effect (here Pockels effect) can change the refractive index as well. Thus, the total refractive variation to distort the optical wave can be described as [24]

$$\Delta\left(\frac{1}{\epsilon}\right) = \mathbf{r} \cdot \mathbf{E}_{\text{RF}} + \mathbf{p} : \mathbf{S} \approx \mathbf{p} : \mathbf{S}, \quad (33)$$

where \mathbf{r} and \mathbf{p} are electrooptic and photoelastic tensors, respectively. We should note that the RF signal generated through second order nonlinearity can interact with Stokes (pump) and thus create a pump (Stokes) wave ($A_p \propto A_s \Psi$). However with more details shown in

the appendix A, we neglect the impact of electrooptic effect and perturbation of optical wave by the RF signal ($\Psi\Delta\tilde{\mathbf{e}}_{2,i}$) and assume it is negligible, therefore, the whole of the RF power transformed into acoustic domain through the electromechanical effect. Then, total electric field based on the perturbation theory can be written as follows

$$\begin{aligned}\mathbf{E} &= A_p\tilde{\mathbf{e}}_p + A_s b\Delta\tilde{\mathbf{e}}_{1,p} + A_s\Psi\Delta\tilde{\mathbf{e}}_{2,p} + A_s\tilde{\mathbf{e}}_s + A_p b^*\Delta\tilde{\mathbf{e}}_{1,s} \\ &+ A_p\Psi^*\Delta\tilde{\mathbf{e}}_{2,s} + c.c. \\ &= A_p\tilde{\mathbf{e}}_p + A_s b\Delta\tilde{\mathbf{e}}_{1,p} + A_s\tilde{\mathbf{e}}_s + A_p b^*\Delta\tilde{\mathbf{e}}_{1,s} + c.c.,\end{aligned}\quad (34)$$

where

$$\Delta\tilde{\mathbf{e}}_i = \Delta\mathbf{e}_i(x, y)e^{i(\beta_i z - \omega_i t)}. \quad (35)$$

With this assumption, the formulation of governing envelope equations of pump and Stokes for non-centrosymmetric is the same with Eq. (3) and Eq. (4) with the differences in the results of b and $\tilde{\mathbf{u}}$. In non-centrosymmetric due to piezoelectric effect the acoustic mode profile and the envelope can be different from those in a centrosymmetric material.

D. Coupled Mode Equations

Assuming equations of (3), (4), (14) and (28) the general coupled mode equations for optical, piezopotential and acoustic can be obtained. Depending on the presence and/or strength of acoustic and piezopotential envelopes, three different coupled mode interactions are conceivable. The corresponding envelope equations of each case is tabulated in Table 1.

Table.1: The General Coupled Mode Equations

SBS [7]	EBS	ERSBS
$\frac{\partial A_p}{\partial z} = \frac{-i\omega_p \tilde{Q}_p}{\mathcal{P}_p} A_s b$	$\frac{\partial A_p}{\partial z} = \frac{-i\omega_p \tilde{Q}_p}{\mathcal{P}_p} A_s b$	$\frac{\partial A_p}{\partial z} = \frac{-i\omega_p \tilde{Q}_p}{\mathcal{P}_p} A_s b$
$\frac{\partial A_s}{\partial z} = \frac{-i\omega_s \tilde{Q}_s}{\mathcal{P}_s} A_p b^*$	$\frac{\partial A_s}{\partial z} = \frac{-i\omega_s \tilde{Q}_s}{\mathcal{P}_s} A_p b^*$	$\frac{\partial A_s}{\partial z} = \frac{-i\omega_s \tilde{Q}_s}{\mathcal{P}_s} A_p b^*$
$\frac{\partial b}{\partial z} + \alpha_{ac} b = \frac{-i\Omega \tilde{Q}_b}{\mathcal{P}_{ac}} A_p A_s^*$	$\frac{\partial b}{\partial z} + \alpha_{ac} b = \frac{-i\Omega \tilde{Q}_{1,piezo}}{\mathcal{P}_{ac}} \frac{\partial \Psi}{\partial z} + \frac{-i\Omega \tilde{Q}_{2,piezo}}{\mathcal{P}_{ac}} \Psi$	$\frac{\partial b}{\partial z} + \alpha_{ac} b = \frac{-i\Omega \tilde{Q}_b}{\mathcal{P}_{ac}} A_p A_s^* + \frac{-i\Omega \tilde{Q}_{1,piezo}}{\mathcal{P}_{ac}} \frac{\partial \Psi}{\partial z} + \frac{-i\Omega \tilde{Q}_{2,piezo}}{\mathcal{P}_{ac}} \Psi$
	$\frac{\partial \Psi}{\partial z} M_{RF}^{(1)} + \Psi M_{RF}^{(2)} = \frac{\partial b}{\partial z} M_{RF}^{(3)} + b M_{RF}^{(4)}$	$\frac{\partial \Psi}{\partial z} M_{RF}^{(1)} + \Psi M_{RF}^{(2)} = \frac{\partial b}{\partial z} M_{RF}^{(3)} + b M_{RF}^{(4)}$

The first case, is when there is no external injection of acoustic waves through the IDT. Thus, conventional SBS takes place. The second case refers to the situation that IDT induces power and its corresponding acoustic power is much stronger than that produced via pump-Stokes interactions. We call this, electromechanically induced Brillouin scattering (EBS). Finally the third case describes the situation that IDT is on and its induced acoustic signal is comparable with that generated via pump-Stokes interactions, a scenario that we call Electromechanically Reinforced SBS (ERSBS). In deriving the following differential equation for the envelopes, we note that \mathcal{P}_{Loss} is assumed to be zero ($\mathcal{P}_{Loss}=0$).

E. Deriving the Power Conversion Equations

We begin with Eq.14 and rearrangement of Eq. (14)

$$\frac{\partial b}{\partial z} = -b \frac{M_{RF}^{(4)}}{M_{RF}^{(3)}} + \frac{\partial \Psi}{\partial z} \frac{M_{RF}^{(1)}}{M_{RF}^{(3)}} + \Psi \frac{M_{RF}^{(2)}}{M_{RF}^{(3)}}. \quad (36)$$

Then, by substituting in Eq. (28), the acoustic envelope is

$$b = \gamma_1 A_p A_s^* + \gamma_2 \frac{\partial \Psi}{\partial z} + \gamma_3 \Psi, \quad (37)$$

where γ_i (i=1,2,3) are

$$\begin{aligned}\gamma_1 &= \frac{-i\Omega \tilde{Q}_b}{\left(\alpha_{ac} - \frac{M_{RF}^{(4)}}{M_{RF}^{(3)}}\right) \mathcal{P}_{ac}}, \\ \gamma_2 &= \left(\frac{-i\Omega \tilde{Q}_{1,piezo}}{\left(\alpha_{ac} - \frac{M_{RF}^{(4)}}{M_{RF}^{(3)}}\right) \mathcal{P}_{ac}} - \frac{M_{RF}^{(1)}}{M_{RF}^{(3)} \left(\alpha_{ac} - \frac{M_{RF}^{(4)}}{M_{RF}^{(3)}}\right)} \right), \\ \gamma_3 &= \left(\frac{-i\Omega \tilde{Q}_{2,piezo}}{\left(\alpha_{ac} - \frac{M_{RF}^{(4)}}{M_{RF}^{(3)}}\right) \mathcal{P}_{ac}} - \frac{M_{RF}^{(2)}}{M_{RF}^{(3)} \left(\alpha_{ac} - \frac{M_{RF}^{(4)}}{M_{RF}^{(3)}}\right)} \right),\end{aligned}\quad (38)$$

By substitution Eq. (37) in Eq. (3) and Eq. (4) we have

$$\frac{\partial A_p}{\partial z} = -\frac{i\omega_p \tilde{Q}_p}{\mathcal{P}_p} b A_s = -\frac{i\omega_p \tilde{Q}_p}{\mathcal{P}_p} \left[\gamma_1 A_p A_s^* + \gamma_2 \frac{\partial \Psi}{\partial z} + \gamma_3 \Psi \right] A_s, \quad (39)$$

$$\frac{\partial A_s}{\partial z} = -\frac{i\omega_s \tilde{Q}_s}{\mathcal{P}_s} A_p b^* = -\frac{i\omega_s \tilde{Q}_s}{\mathcal{P}_s} \left[\gamma_1 A_p A_s^* + \gamma_2 \frac{\partial \Psi}{\partial z} + \gamma_3 \Psi \right]^* A_p, \quad (40)$$

where $P_i = (-1)^\xi \mathcal{P}_i |A_i|^2$ (Where ξ is equal to zero and one for forward and backward wave, respectively) and

as shown in the appendix $P_{\text{piezo}} \approx \mathcal{P}_{\text{piezo}} |b|^2$, the power differential equation for a lossless medium can be written as follows

$$\frac{\partial P_p}{\partial z} = 2\Re\left\{ \frac{-\Omega\omega_p |\tilde{Q}_b|^2}{(\alpha_{\text{ac}} - \frac{M_{\text{RF}}^{(4)}}{M_{\text{RF}}^{(3)}}) \mathcal{P}_{\text{ac}} \mathcal{P}_p} \right\} \mathcal{P}_p |A_p|^2 |A_s|^2 + 2\Re\left\{ -\frac{i\omega_p \tilde{Q}_p}{\mathcal{P}_p} \gamma_2 \mathcal{P}_p A_p^* A_s \frac{\partial \Psi}{\partial z} \right\} + 2\Re\left\{ -\frac{i\omega_p \tilde{Q}_p}{\mathcal{P}_p} \gamma_3 \mathcal{P}_p A_p^* A_s \Psi \right\}, \quad (41)$$

$$\frac{\partial P_s}{\partial z} = \frac{2\Omega\omega_s |\tilde{Q}_b|^2}{(\alpha_{\text{ac}} - \frac{M_{\text{RF}}^{(4)}}{M_{\text{RF}}^{(3)}}) \mathcal{P}_{\text{ac}} \mathcal{P}_s} \mathcal{P}_s |A_p|^2 |A_s|^2 + 2\Re\left\{ \left(-\frac{i\omega_s \tilde{Q}_s}{\mathcal{P}_s}\right) \left(\gamma_2 \mathcal{P}_s A_p^* A_s \frac{\partial \Psi}{\partial z}\right)^* \right\} + 2\Re\left\{ \left(-\frac{i\omega_s \tilde{Q}_s}{\mathcal{P}_s}\right) \left(\gamma_3 \mathcal{P}_s A_p^* A_s \Psi\right)^* \right\}, \quad (42)$$

$$\frac{\partial P_{\text{piezo}}}{\partial z} = \mathcal{P}_{\text{piezo}} \left(b \frac{\partial b^*}{\partial z} + b^* \frac{\partial b}{\partial z} \right) = 2\mathcal{P}_{\text{piezo}} \Re\left\{ b^* \frac{\partial b}{\partial z} \right\}. \quad (43)$$

As shown in the appendix C, the two terms of $A_p^* A_s \frac{\partial \Psi}{\partial z}$

and $A_p^* A_s \Psi$ can be written as

$$\begin{aligned} A_p^* A_s \Psi &\approx \sigma_1 P_{\text{piezo}} P_p - \sigma_1 P_{\text{piezo}} P_s + \sigma_2 P_{\text{piezo}} P_p^2 + \sigma_2 P_{\text{piezo}} P_s^2 - 2\sigma_2 P_{\text{piezo}} P_p P_s + \sigma_3 P_{\text{piezo}}, \\ A_p^* A_s \frac{\partial \Psi}{\partial z} &\approx \tau_1 P_{\text{piezo}} P_p - \tau_1 P_{\text{piezo}} P_s + \tau_2 P_{\text{piezo}} P_p^2 + \tau_2 P_{\text{piezo}} P_s^2 - 2\tau_2 P_{\text{piezo}} P_p P_s, \end{aligned} \quad (44)$$

where σ_i and τ_i are piezo-coefficients as

$$\begin{aligned} \sigma_1 &= \frac{1}{\mathcal{P}_{\text{piezo}}} \left(-\frac{M_{\text{RF}}^{(4)}}{M_{\text{RF}}^{(2)}} \left(\frac{\gamma_2 \gamma_4 M_{\text{RF}}^{(4)}}{\gamma_1 M_{\text{RF}}^{(2)}} + \frac{\gamma_3 \gamma_4}{\gamma_1} \left(\frac{M_{\text{RF}}^{(3)} - \frac{M_{\text{RF}}^{(1)} M_{\text{RF}}^{(4)}}{M_{\text{RF}}^{(2)}}}{M_{\text{RF}}^{(2)}} \right) \right)^* + \left(\gamma_4 \left(\frac{M_{\text{RF}}^{(3)} - \frac{M_{\text{RF}}^{(1)} M_{\text{RF}}^{(4)}}{M_{\text{RF}}^{(2)}}}{M_{\text{RF}}^{(2)}} \right) \right) \left(\frac{1}{\gamma_1} - \frac{\gamma_3 M_{\text{RF}}^{(4)}}{\gamma_1 M_{\text{RF}}^{(2)}} \right)^* \right), \\ \sigma_2 &= \frac{-1}{\mathcal{P}_{\text{piezo}}} \left(\frac{\gamma_2 \gamma_4 M_{\text{RF}}^{(4)}}{\gamma_1 M_{\text{RF}}^{(2)}} + \frac{\gamma_3 \gamma_4}{\gamma_1} \left(\frac{M_{\text{RF}}^{(3)} - \frac{M_{\text{RF}}^{(1)} M_{\text{RF}}^{(4)}}{M_{\text{RF}}^{(2)}}}{M_{\text{RF}}^{(2)}} \right) \right)^* \left(\gamma_4 \left(\frac{M_{\text{RF}}^{(3)} - \frac{M_{\text{RF}}^{(1)} M_{\text{RF}}^{(4)}}{M_{\text{RF}}^{(2)}}}{M_{\text{RF}}^{(2)}} \right) \right), \\ \sigma_3 &= \frac{1}{\mathcal{P}_{\text{piezo}}} \frac{M_{\text{RF}}^{(4)}}{M_{\text{RF}}^{(2)}} \left(\frac{1}{\gamma_1} - \frac{\gamma_3 M_{\text{RF}}^{(4)}}{\gamma_1 M_{\text{RF}}^{(2)}} \right)^*, \\ \tau_1 &= \frac{1}{\mathcal{P}_{\text{piezo}}} \left(\frac{1}{\gamma_1} - \frac{\gamma_3 M_{\text{RF}}^{(4)}}{\gamma_1 M_{\text{RF}}^{(2)}} \right)^* \left(\gamma_4 \frac{M_{\text{RF}}^{(4)}}{M_{\text{RF}}^{(2)}} \right), \\ \tau_2 &= \frac{1}{\mathcal{P}_{\text{piezo}}} \left(-\left(\frac{\gamma_2 \gamma_4 M_{\text{RF}}^{(4)}}{\gamma_1 M_{\text{RF}}^{(2)}} + \frac{\gamma_3 \gamma_4}{\gamma_1} \left(\frac{M_{\text{RF}}^{(3)} - \frac{M_{\text{RF}}^{(1)} M_{\text{RF}}^{(4)}}{M_{\text{RF}}^{(2)}}}{M_{\text{RF}}^{(2)}} \right) \right) \right)^* \left(\gamma_4 \frac{M_{\text{RF}}^{(4)}}{M_{\text{RF}}^{(2)}} \right). \end{aligned} \quad (45)$$

Also, it is shown that

$$\frac{\partial b}{\partial z} \approx \gamma_4 (P_p - P_s) b, \quad (46)$$

where γ_4 is

$$\gamma_4 = \left(\frac{\gamma_1}{1 - \gamma_3 \frac{M_{\text{RF}}^{(4)}}{M_{\text{RF}}^{(2)}}} \right) \left(\frac{i\omega_p \tilde{Q}_p}{\mathcal{P}_p \mathcal{P}_s} \right) = \frac{\omega_p \Omega |\tilde{Q}_p|^2}{\mathcal{P}_p \mathcal{P}_s \left((\alpha_{\text{ac}} - \frac{M_{\text{RF}}^{(4)}}{M_{\text{RF}}^{(3)}}) \mathcal{P}_{\text{ac}} \right) + (i\Omega \tilde{Q}_{2,\text{piezo}} \frac{M_{\text{RF}}^{(4)}}{M_{\text{RF}}^{(2)}}) + \frac{M_{\text{RF}}^{(2)} \mathcal{P}_{\text{ac}}}{M_{\text{RF}}^{(3)}}} \right). \quad (47)$$

Therefore, the power conversion differential equation can

be expressed as follows

$$\begin{aligned} \frac{\partial P_p}{\partial z} &= -\Upsilon_0 P_p P_s - \Upsilon_1 P_{\text{piezo}} P_p + \Upsilon_1 P_{\text{piezo}} P_s - \Upsilon_2 P_{\text{piezo}} P_p^2 - \Upsilon_2 P_{\text{piezo}} P_s^2 + 2\Upsilon_2 P_{\text{piezo}} P_p P_s - \Upsilon_3 P_{\text{piezo}}, \\ \frac{\partial P_s}{\partial z} &= \Upsilon_0 P_p P_s + \Upsilon_1 P_{\text{piezo}} P_p - \Upsilon_1 P_{\text{piezo}} P_s + \Upsilon_2 P_{\text{piezo}} P_p^2 + \Upsilon_2 P_{\text{piezo}} P_s^2 - 2\Upsilon_2 P_{\text{piezo}} P_p P_s + \Upsilon_3 P_{\text{piezo}}, \\ \frac{\partial P_{\text{piezo}}}{\partial z} &= \Upsilon_{\text{piezo}} P_{\text{piezo}} (P_p - P_s), \end{aligned} \quad (48)$$

where ERSBS (EBS) coefficients Υ_0 and Υ_i ($i=1:3$) are

$$\begin{aligned} \Upsilon_0 &= 2\Re\left\{ \frac{\Omega \omega_p |\tilde{Q}_b|^2}{(\alpha_{\text{ac}} - \frac{M_{\text{RF}}^{(4)}}{M_{\text{RF}}^{(3)}}) \mathcal{P}_{\text{ac}} \mathcal{P}_p \mathcal{P}_s} \right\}, \\ \Upsilon_i &= \Upsilon_{i,p} = 2\Re\left\{ \left(\frac{-i\omega_p \tilde{Q}_p}{\mathcal{P}_p} \right) \tau_i \gamma_2 \right\} + 2\Re\left\{ \left(\frac{-i\omega_p \tilde{Q}_p}{\mathcal{P}_p} \right) \sigma_i \gamma_3 \right\}, \\ \Upsilon_{i,s} &= 2\Re\left\{ \left(-\frac{i\omega_s \tilde{Q}_s}{\mathcal{P}_s} \right) \tau_i^* \gamma_2^* \right\} + 2\Re\left\{ \left(-\frac{i\omega_s \tilde{Q}_s}{\mathcal{P}_s} \right) \sigma_i^* \gamma_3^* \right\} \\ &= 2\Re\left\{ \left(\frac{i\omega_p \tilde{Q}_p}{\mathcal{P}_s} \right)^* \tau_i^* \gamma_2^* \right\} + 2\Re\left\{ \left(\frac{i\omega_p \tilde{Q}_p}{\mathcal{P}_s} \right)^* \sigma_i^* \gamma_3^* \right\} = -\Upsilon_i, \end{aligned} \quad (49)$$

and piezo power loss (Υ_{piezo}) is

$$\Upsilon_{\text{piezo}} = 2\Re\{\gamma_4\}. \quad (50)$$

V. DISCUSSION

The mutual effect of the RF signal - excited in a piezoelectric material by the IDT - and the optical waves can be explained by a direct electrooptic effect, together with an indirect acoustic mediated process. As shown in Fig. 2, acoustic waves propagated in the structure are influenced by the strength of optical waves through SBS or other optomechanical phenomena such as piezo optomechanical cavity. The acoustic wave may also be excited externally by IDT through piezoelectric effect separately. In our study, we showed how an acoustic wave excited by pump and Stokes waves through SBS effect and externally injection of phonon by IDT contribute in power conversion from pump to Stokes. We here neglect the electrooptic effect for the SBS process because the gener-

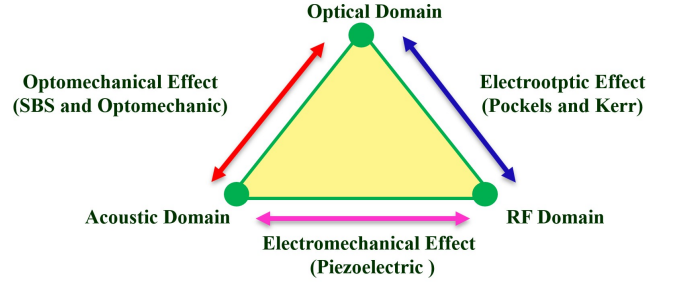


FIG. 2. Conversion process of optic, acoustic and RF domains.

ated RF signal through $\chi^{(2)}$ effect is weak as shown in appendix A. Then, we move through the indirect interaction between the RF signal and the optical waves of Fig. 2, the two step process which we call piezo-optomechanical interaction. The electrooptic side for our research is disconnected. Figure 3 shows the general SBS process for the intra mode coupling case. Intra mode is referred carrying of the identical mode of optical waves while inter mode is for different modes. Within the backward intra mode SBS (Fig. 3 (a)) the excited acoustic modes have large-wavenumbers and strong variations along the waveguide direction, which resemble them to a nearly longitudinal mode. In forward intra mode SBS (Fig. 3 (b)) the Stokes is co-propagates of optical and acoustics wave. Therefore, due to conservation of momentum, acoustic modes occur near the acoustic propagation constant $q \approx 0$ where the acoustic modes do not propagate along the waveguide axis any more (they possess the form of shear waves). Thus, the modes have strong transverse components. Without considering the type of scattering, energy and momentum conservation laws

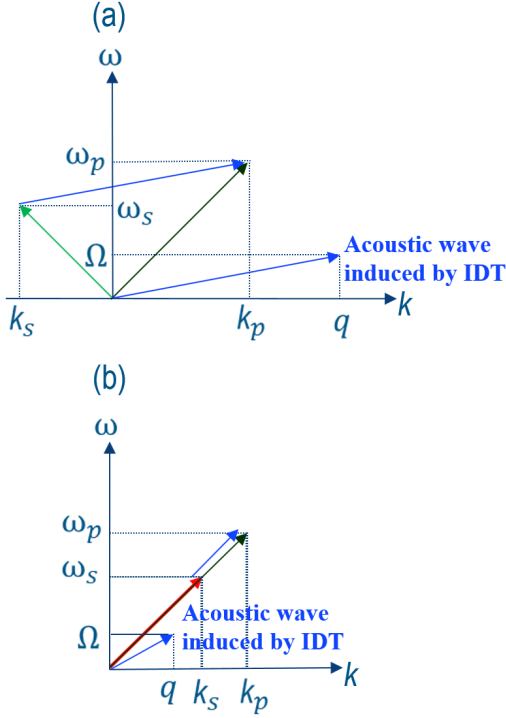


FIG. 3. The dispersion diagram of the ERSBS (a) Backward (b) Forward process. Black and green (red) arrows indicate pump and backward (forward) Stokes, respectively and Blue arrows shows the acoustic dispersion diagram.

make a constraint to prepare the phase-matching condition on the opto-acoustic interactions. The distinguishing phase-matching conditions result in different sets of coupled wave equations with unique dynamics. For reinforcing the SBS, an acoustic wave with same frequency (Ω) and wave vector (q) as shown in Fig. 3 externally is induced to the waveguide by IDT, which enhances the excited acoustic wave due to pump-Stokes interactions.

VI. CASE STUDY: ERSBS IN GALLIUM ARSENIDE NANOWIRE

We here solve the coupled mode equations in Eq. (48) from numerical approaches. The applied method is different depend on the forward or to study the backward ERSBS process in a GaAs nanowire. In this study, we focus on backward ERSBS where pump and Stokes are counter propagated along the waveguide which leads to differential equations with two points boundary value problem. A backward ERSBS in a GaAs nanowire with a cross section of 500 nm (width) and 220 nm (height), and refractive index of 3.37 at the wavelength 1550 nm is demonstrated. The fundamental optical mode and acoustic and piezopotential modes at the corresponding frequency are depicted in Fig. 4.

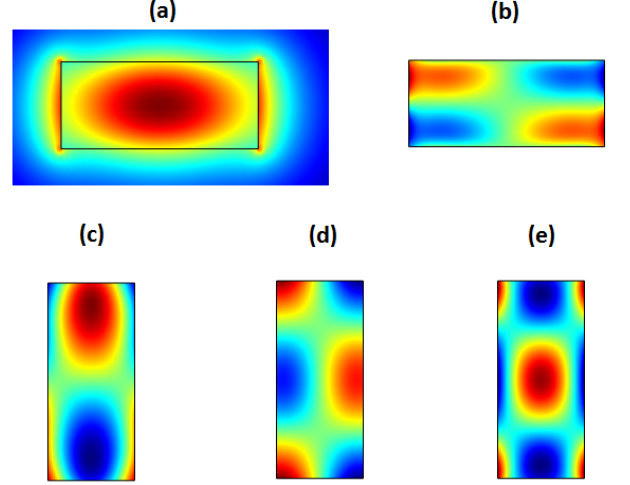


FIG. 4. Mode profiles of norm of optical waves ($|\mathbf{E}|$) at 1550 nm (a) piezopotential mode ($\tilde{\phi}$) at 66.05 [GRad/s] (b) acoustic mode in x direction ($\tilde{\mathbf{u}}_x$) (c) acoustic mode in y direction ($\tilde{\mathbf{u}}_y$) (d) acoustic mode in z direction ($\tilde{\mathbf{u}}_z$) (e) for a GaAs waveguide with a cross section of 220 nm \times 500 nm.

First, the SBS gain without IDT is investigated. As shown in Fig. 5, a maximum gain of $7957.26 \text{ W}^{-1}\text{m}^{-1}$ occurs at $\Omega = 66.05$ [GRad/s]. Next, the IDT becomes activated and launches a designed piezoelectric power to the structure. It must be mentioned that the acoustic loss coefficient ($\alpha_{ac} = \frac{q}{Q_m}$) is calculated by assuming a mechanical Q factor (Q_m) of 1000 with $q = 1.51 \times 10^7$ Rad/m.

It can be observed from Table 2 that SBS gain from interaction of pump and Stokes has dramatically reduced due to presence of piezoelectric effect through Υ_0 coefficient. We can recognize four types of losses in piezoelectric material including acoustic loss (α_{ac}) from purely mechanical structural damping, coupling loss of electromechanical process (α_{EIM}), dielectric loss because of the material polarization and conduction loss due to electrical energy dissipation or Ohm law where we neglect the dielectric and conduction losses in this study[25, 26]. In this regard, the electromechanical loss (α_{EIM}) can be derived by a rearrangement of Eq.(14) as follows

$$\frac{\partial b}{\partial z} + \alpha_{EIM} b = \frac{M_{RF}^{(1)}}{M_{RF}^{(3)}} \frac{\partial \Psi}{\partial z} + \frac{M_{RF}^{(2)}}{M_{RF}^{(3)}} \Psi, \quad (51)$$

where α_{EIM} is equal to $\frac{M_{RF}^{(4)}}{M_{RF}^{(3)}}$. This impact is presented as loss for the proposed structure and reducing the parameter Υ_0 significantly. This ratio takes a complex value with large imaginary part for the proposed acoustic mode. The real part of this ratio is $-6.033 \times 10^{-8} [\text{m}^{-1}]$, while the imaginary part reaches $-2.93 \times 10^7 [\text{m}^{-1}]$, which leads a significant reduction of the Υ_0 .

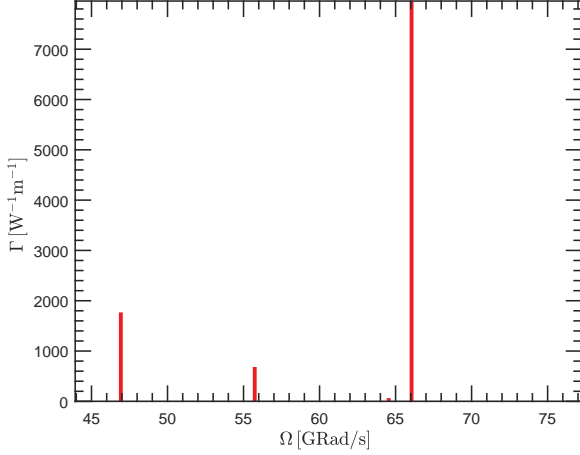


FIG. 5. Backward SBS gain without IDT.

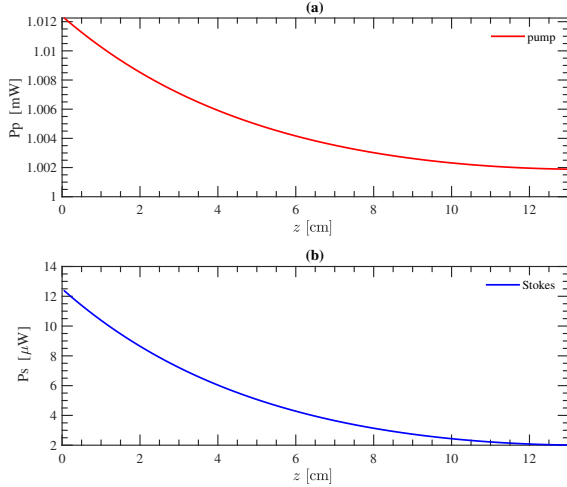


FIG. 6. Power conversion without IDT with initial power values of (a) pump, (b) Stokes and of 1.012 mW and 2 μ W with a waveguide length of 13 cm.

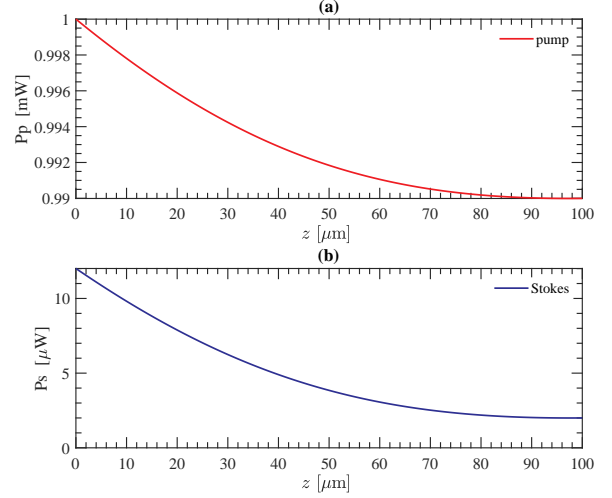


FIG. 7. Power conversion with IDT with initial power values of (a) pump, (b) Stokes and piezoelectric of 1 mW, 2 μ W and 1 μ W with a waveguide length of 100 μ m.

The power conversion for both scenarios (i.e. SBS in the presence and absence of IDT) are shown in Fig. 6 and Fig. 7. It is assumed that the initial values for the pump and piezoelectric power are about 1 mW and 1 μ W at the beginning of the waveguide respectively while the initial value of Stokes power at the end of waveguide with length of 13 cm for conventional SBS (without IDT) and a length of 100 μ m in the present of IDT is equal to 2 μ W. It can be seen that the Stokes is amplified exponentially through the backward direction while the pump is depleted in the forward direction. Although by applying the IDT the Υ_0 coefficient will reduce drastically, however; the parameters of Υ_i ($i=1,2,3$) tabulated in table 2, play a key role in Stokes amplification as shown in Fig. 7. As can be seen larger Stokes amplification in this situation occurs compared with conventional SBS process; this reduces the scale of the integrated Brillouin chip about two order of magnitude (from 13 cm to 100 μ m in this case).

Table.2: The values of ERSBS coefficients of governing power equation for the proposed mode

State	Angular frequency [GRad/s]	Υ [$\text{W}^{-1}\text{m}^{-1}$]	Υ_0 [$\text{W}^{-1}\text{m}^{-1}$]	Υ_1 [$\text{W}^{-1}\text{m}^{-1}$]	Υ_2 [$\text{W}^{-2}\text{m}^{-1}$]	Υ_3 [m^{-1}]
ERSBS	66.05	-1.0293×10^4	0.00302	1.8947×10^8	34.0976	-6.6448×10^8

VII. CONCLUSION

To sum up, we theoretically demonstrated Brillouin scattering in a piezoelectric medium in the presence of externally injection of acoustic phonons. We derived the governing equations corresponding to this electromechanical interaction. It was shown how the envelope of the

excited acoustic mode varies due to piezoelectricity and the intensity of the externally injected wave. We observed that the piezoelectric forces play a critical role in the optomechanical interactions. These forces have been influenced on the the piezoelectric overlap integral ($\tilde{Q}_{i,\text{piezo}}(i = 1, 2)$) through the projection of the excited acoustic mode on the piezoelectric forces. The power con-

version between pump and Stokes were obtained and its characteristics were compared with SBS governing equations in non-piezoelectric waveguides. As a case study, the method investigated in GaAs nanowire. It was found

that Stokes wave can be amplified in few hundred micrometer instead of centimeter scale in the conventional integrated SBS chip.

-
- [1] R. W. Boyd, *Nonlinear optics* (Academic press, 2020).
- [2] L. Brillouin, Diffusion of light and x-rays by a transparent homogeneous body, *Ann. Phys* 17, 88 (1922).
- [3] L. Mandelstam, Light scattering by inhomogeneous media, *Zh. Russ. Fizhim. Ova* 58, 381 (1926).
- [4] B. J. Eggleton, C. G. Poulton, P. T. Rakich, M. J. Steel, and G. Bahl, Brillouin integrated photonics, *Nature Photonics* 13, 664 (2019).
- [5] E. Garmire, Perspectives on stimulated Brillouin scattering, *New Journal of Physics* 19, 011003 (2017).
- [6] P. T. Rakich, C. Reinke, R. Camacho, P. Davids, and Z. Wang, Giant enhancement of stimulated Brillouin scattering in the subwavelength limit, *Physical Review X* 2, 011008 (2012).
- [7] C. Wolff, M. J. Steel, B. J. Eggleton, and C. G. Poulton, Stimulated Brillouin scattering in integrated photonic waveguides: Forces, scattering mechanisms, and coupled-mode analysis, *Physical Review A* 92, 013836 (2015).
- [8] H. Shin, W. Qiu, R. Jarecki, J. A. Cox, R. H. Olsson, A. Starbuck, Z. Wang, and P. T. Rakich, Tailorable stimulated Brillouin scattering in nanoscale silicon waveguides, *Nature communications* 4, 1 (2013).
- [9] C. G. Poulton, R. Pant, and B. J. Eggleton, Acoustic confinement and stimulated Brillouin scattering in integrated optical waveguides, *JOSA B* 30, 2657 (2013).
- [10] R. Van Laer, B. Kuyken, D. Van Thourhout, and R. Baets, Interaction between light and highly confined hypersound in a silicon photonic nanowire, *Nature Photonics* 9, 199 (2015).
- [11] S. R. Mirnaziry, C. Wolff, M. Steel, B. J. Eggleton, and C. G. Poulton, Stimulated Brillouin scattering in silicon/chalcogenide slot waveguides, *Optics express* 24, 4786 (2016).
- [12] F. Gyger, J. Liu, F. Yang, J. He, A. S. Raja, R. N. Wang, S. A. Bhave, T. J. Kippenberg, and L. Thevenaz, Observation of stimulated Brillouin scattering in silicon nitride integrated waveguides, *Physical review letters* 124, 013902 (2020).
- [13] R. Pant, C. G. Poulton, D.-Y. Choi, H. Mcfarlane, S. Hile, E. Li, L. Thevenaz, B. Luther-Davies, S. J. Madden, and B. J. Eggleton, On-chip stimulated Brillouin scattering, *Optics express* 19, 8285 (2011).
- [14] Q. Liu, H. Li, and M. Li, Electromechanical Brillouin scattering in integrated optomechanical waveguides, *Optica* 6, 778 (2019).
- [15] E. A. Kittlaus, W. M. Jones, P. T. Rakich, N. T. Otterstrom, R. E. Muller, and M. Rais-Zadeh, Electrically driven acousto-optics and broadband non-reciprocity in silicon photonics, *Nature Photonics* 15, 43 (2021).
- [16] F. M. Mayor, W. Jiang, C. J. Sarabalis, T. P. McKenna, J. D. Witmer, and A. H. Safavi-Naeini, Gigahertz phononic integrated circuits on thin-film lithium niobate on sapphire, *Physical Review Applied* 15, 014039 (2021).
- [17] L. Shao, M. Yu, S. Maity, N. Sinclair, L. Zheng, C. Chia, A. Shams-Ansari, C. Wang, M. Zhang, K. Lai, et al., Microwave-to-optical conversion using lithium niobate thin-film acoustic resonators, *Optica* 6, 1498 (2019).
- [18] Y. D. Dahmani, C. J. Sarabalis, W. Jiang, F. M. Mayor, and A. H. Safavi-Naeini, Piezoelectric transduction of a wavelength-scale mechanical waveguide, *Physical Review Applied* 13, 024069 (2020).
- [19] K. C. Balram, M. I. Davanco, B. R. Ilic, J.H. Kyhm, J. D. Song, and K. Srinivasan, Acousto-optic modulation and optoacoustic gating in piezo-optomechanical circuits, *Physical review applied* 7, 024008 (2017).
- [20] W. Jiang, C. J. Sarabalis, Y. D. Dahmani, R. N. Patel, F. M. Mayor, T. P. McKenna, R. Van Laer, and A. H. Safavi-Naeini, Efficient bidirectional piezo-optomechanical transduction between microwave and optical frequency, *Nature communications* 11, 1 (2020).
- [21] M. Wu, E. Zeuthen, K. C. Balram, and K. Srinivasan, Microwave-to-optical transduction using a mechanical supermode for coupling piezoelectric and optomechanical resonators, *Physical Review Applied* 13, 014027 (2020).
- [22] B. A. Auld, *Acoustic fields and waves in solids* (,1973).
- [23] N. A. Shepelin, P. C. Sherrell, E. N. Skountzos, E. Goudeli, J. Zhang, V. C. Lussini, B. Imtiaz, K. A. S. Usman, G. W. Dicoski, J. G. Shapter, et al., Interfacial piezoelectric polarization locking in printable Ti3C2Tx MXene-fluoropolymer composites, *Nature communications* 12, 1 (2021).
- [24] I. Biaggio, Nonlocal contributions to degenerate four wave mixing in noncentrosymmetric materials, *Physical review letters* 82, 193 (1999).
- [25] González, Amador M., et al. "Revisiting the characterization of the losses in piezoelectric materials from impedance spectroscopy at resonance." *Materials* 9.2 (2016): 72
- [26] Z. Yuan, S. O. Ural, and K. Uchino, Loss factor characterization methodology for piezoelectric ceramics, in *IOP Conference Series. Materials Science and Engineering* (Online), Vol. 18 (2011).
- [27] M. Lax and D. Nelson, Electrodynamics of elastic pyroelectrics, *Physical Review B* 13, 1759 (1976).
- [28] D. Nelson and M. Lax, Linear elasticity and piezoelectricity in pyroelectrics, *Physical Review B* 13, 1785 (1976).
- [29] B. D. Zaitsev and I. E. Kuznetsova, The energy density and power flow of acoustic waves propagating in piezoelectric materials, *IEEE transactions on ultrasonics, ferroelectrics, and frequency control* 50, 1762 (2003).

VIII. APPENDIX

A. RF wave generated via optical interactions

The pump and Stokes interaction in a noncentrosymmetric material can generate RF wave due to diife DFG. In the context of SBS, We are well motivated for those RF signal that possess a frequency match to the Brillouin frequency Ω . The electric displacement field in non-centrosymmetric material for this scenario can be expressed by [27, 28]

$$\mathbf{D}_{\text{RF}} = \epsilon \cdot \mathbf{E}_{\text{RF}} + \mathbf{e}^{\text{F}} : \mathbf{S} + \epsilon_0 \chi^{(2)} \cdot \mathbf{E}_{\text{p}} \mathbf{E}_{\text{s}}^* + c.c., \quad (52)$$

where \mathbf{e}^{F} is [28]

$$\mathbf{e}^{\text{F}} = \mathbf{e} - \epsilon_0 \chi^{(2)} \cdot \mathbf{E}_{\text{p}} \mathbf{E}_{\text{p}}^* - \epsilon_0 \chi^{(2)} \cdot \mathbf{E}_{\text{s}} \mathbf{E}_{\text{s}}^* \approx \mathbf{e}. \quad (53)$$

Before investigating the contribution of second order non-linearity $\chi^{(2)}$, We review the phase matching condition in naoncentro-symmetric material when DFG take places. There are three wave numbers that play role in this situations; i.e. Pump and Stokes wavenumbers k_{p} , k_{s} and and that of their nonlinear process, k_{DFG} . Phase matching occurs when

$$\Delta k = k_{\text{p}} \pm k_{\text{s}} - k_{\text{DFG}} = 0, \quad (54)$$

If we expand the wave numbers, we have

$$\Delta k = \frac{\omega_{\text{p}} n(\omega_{\text{p}})}{c} \pm \frac{\omega_{\text{s}} n(\omega_{\text{s}})}{c} - \frac{\Omega_{\text{RF}} n(\Omega_{\text{RF}})}{c} = 0, \quad (55)$$

Δk becomes nonzero in a non-centrosymmetric material through DFG process for backward scattering while under certain circumstances in forward scattering it can be nullified to achieve phase matching condition. A non zero Δk thus, can drastically reduce the power conversion between pump and Stokes, hence a weak RF envelope is generated through their interaction. Even with the assumption of phase matching condition, the value of $\epsilon_0 \chi^{(2)} \cdot \mathbf{E}_{\text{p}} \mathbf{E}_{\text{s}}^*$ through the electrooptic (EO) effect is very small in comparison with the piezoelectric stress tensor term $\mathbf{e} : \mathbf{S}$ [24]. With that, we can neglect the corresponding RF signal from DFG and in general EO effect.

B. Energy density and power flow in a piezoelectric medium

In general, the total energy of a propagating medium is summation of kinetic and stored (potential) energy

$$\mathcal{W}_{\text{tot}} = \mathcal{W}_{\text{kinetic}} + \mathcal{W}_{\text{stored}}, \quad (56)$$

where kinetic energy is:

$$\mathcal{W}_{\text{kinetic}} = -\frac{\Omega^2}{2} \int \rho (\tilde{\mathbf{u}}^* \cdot \tilde{\mathbf{u}}) dv + c.c., \quad (57)$$

and stored energy can be divided to mechanical and electrical energy.

$$\mathcal{W}_{\text{stored}} = \mathcal{W}_{\text{tot}}^{\text{M}} + \mathcal{W}_{\text{tot}}^{\text{El}}. \quad (58)$$

The total time-average density of stored mechanical energy $\mathcal{W}_{\text{tot}}^{\text{M}}$ and electrical energy $\mathcal{W}_{\text{tot}}^{\text{El}}$ can be expressed as [22]

$$\begin{aligned} \mathcal{W}_{\text{tot}}^{\text{M}} &= \int (\mathbf{T}_{\text{tot}}^{\text{piezo}} : \mathbf{S}^*) dv, \\ \mathcal{W}_{\text{tot}}^{\text{El}} &= \int (\mathbf{D}_{\text{RF}}^* \cdot \mathbf{E}_{\text{RF}}) dv, \end{aligned} \quad (59)$$

where $\mathbf{T}_{\text{tot}}^{\text{piezo}} = \mathbf{c} : \mathbf{S} - \mathbf{e} \cdot \mathbf{E}_{\text{RF}}$ is the stress. It must be noted that the energy and power differs from Ref [22] by a factor of $\frac{1}{2}$, is due to our convention used in Eq. (2). By substitution of Eq. (7) and Eq. (19) in Eq. (59) we have:

$$\begin{aligned} \mathcal{W}_{\text{tot}}^{\text{M}} &= \int \{(\mathbf{c} : \mathbf{S}) : \mathbf{S}^* - (\mathbf{e} \cdot \mathbf{E}_{\text{RF}}) : \mathbf{S}^*\} dv \\ &= \mathcal{W}_{\text{pure}}^{\text{M}} + \mathcal{W}^{\text{MEI}}, \\ \mathcal{W}_{\text{tot}}^{\text{El}} &= \int \{(\epsilon \cdot \mathbf{E}_{\text{RF}})^* \cdot \mathbf{E}_{\text{RF}} + (\mathbf{e} : \mathbf{S})^* \cdot \mathbf{E}_{\text{RF}}\} dv \\ &= \mathcal{W}_{\text{pure}}^{\text{El}} + \mathcal{W}^{\text{EIM}}, \end{aligned} \quad (60)$$

where,

$$\begin{aligned} \mathcal{W}_{\text{pure}}^{\text{M}} &= \int \{-(\mathbf{c} : \mathbf{S}) : \mathbf{S}^*\} dv, \\ \mathcal{W}_{\text{pure}}^{\text{El}} &= \int \{(\mathbf{e} \cdot \mathbf{E}_{\text{RF}})^* \cdot \mathbf{E}_{\text{RF}}\} dv, \\ \mathcal{W}^{\text{MEI}} &= \int \{-(\mathbf{e} \cdot \mathbf{E}_{\text{RF}}) : \mathbf{S}^*\} dv, \\ \mathcal{W}^{\text{EIM}} &= \int \{(\mathbf{e} : \mathbf{S})^* \cdot \mathbf{E}_{\text{RF}}\} dv, \end{aligned} \quad (61)$$

and energy in terms of integral form is

$$\begin{aligned} \mathcal{W}^{\text{MEI}} &= \int (\mathbf{e} \cdot \nabla(\Psi \tilde{\phi})) : \nabla(b \tilde{\mathbf{u}}^*) dv + c.c., \\ \mathcal{W}^{\text{EIM}} &= - \int ((\mathbf{e} : \nabla(b \tilde{\mathbf{u}}))^* \cdot \nabla(\Psi \tilde{\phi})) dv + c.c.. \end{aligned} \quad (62)$$

It can be observed that mechanical energy (electrical energy) are divided into pure mechanical (electrical) and mechano-electrical (electromechanical) energy. The densities of mechano-electrical and electromechanical energies in arbitrary piezoelectric media are always equal in absolute value and have opposite signs [29]. which means

$$|\mathcal{W}^{\text{MEI}}| = -|\mathcal{W}^{\text{EIM}}|. \quad (63)$$

Now the piezoelectric Poynting vector $\mathbf{P}_{\text{piezo}}$ with quasi

static approximation including acoustic and RF parts is calculated by [22]:

$$P_{\text{piezo}} = \int (-\mathbf{V}^* \cdot \mathbf{T}_{\text{tot}}^{\text{piezo}} + \Phi(-i\Omega \mathbf{D}_{\text{RF}})^*) \cdot \mathbf{d}s + c.c., \quad (64)$$

and after an expansion, it is

$$\begin{aligned} P_{\text{piezo}} = & |b|^2 \left(\int (-\tilde{\mathbf{v}}^* \cdot (\mathbf{c} : \nabla \tilde{\mathbf{u}})) \cdot \mathbf{d}s \right) + b^* \frac{\partial b}{\partial z} \left(\int (-\tilde{\mathbf{v}}^* \cdot (\hat{\mathbf{a}}_z \cdot (\mathbf{c} : \tilde{\mathbf{u}}))) \cdot \mathbf{d}s \right) + b^* \Psi \left(\int (-\tilde{\mathbf{v}}^* \cdot (\mathbf{e} \cdot \nabla \tilde{\phi})) \cdot \mathbf{d}s \right) \\ & + b^* \frac{\partial \Psi}{\partial z} \left(\int (-\tilde{\mathbf{v}}^* \cdot (\hat{\mathbf{a}}_z \cdot (\mathbf{e} : \tilde{\phi}))) \cdot \mathbf{d}s \right) + |\Psi|^2 \left(\int -i\Omega \tilde{\phi} (\epsilon \cdot \nabla \tilde{\phi})^* \cdot \mathbf{d}s \right) + \Psi \frac{\partial \Psi^*}{\partial z} \left(\int (\hat{\mathbf{a}}_z \cdot (\epsilon : \tilde{\phi})^*) \cdot \mathbf{d}s \right) \\ & + \Psi b^* \left(\int (\mathbf{r} : \nabla \tilde{\mathbf{u}})^* \cdot \mathbf{d}s \right) + \Psi \frac{\partial b^*}{\partial z} \left(\int (\hat{\mathbf{a}}_z \cdot (\mathbf{r} : \tilde{\mathbf{u}}))^* \cdot \mathbf{d}s \right) + c.c.. \end{aligned} \quad (65)$$

It is assumed that $b(\mathbf{c} : \nabla \tilde{\mathbf{u}}) \gg \frac{\partial b}{\partial z}(\hat{\mathbf{a}}_z \cdot (\mathbf{c} : \tilde{\mathbf{u}}))$. This approximation is also noted in [7], and subsequently $\Psi(\mathbf{e} \cdot \nabla \tilde{\phi}) \gg \frac{\partial \Psi}{\partial z}(\hat{\mathbf{a}}_z \cdot (\mathbf{e} : \tilde{\phi}))$. Therefore, we neglect it in calculating the piezoelectric power.

$\Psi(\mathbf{e} \cdot \nabla \tilde{\phi}) \gg \frac{\partial \Psi}{\partial z}(\hat{\mathbf{a}}_z \cdot (\mathbf{e} : \tilde{\phi}))$. Therefore, we neglect it in calculating the piezoelectric power.

$$\begin{aligned} P_{\text{piezo}} \approx & |b|^2 \left(\int (-\tilde{\mathbf{v}}^* \cdot (\mathbf{c} : \nabla \tilde{\mathbf{u}})) \cdot \mathbf{d}s \right) + b^* \Psi \left(\int (-\tilde{\mathbf{v}}^* \cdot (\mathbf{e} \cdot \nabla \tilde{\phi})) \cdot \mathbf{d}s \right) + |\Psi|^2 \left(\int \left(-i\Omega \tilde{\phi} ((\epsilon \cdot \nabla \tilde{\phi})^*) \cdot \mathbf{d}s \right) \right) \\ & + \Psi b^* \left(\int (-i\Omega \tilde{\phi} (\mathbf{r} : \nabla \tilde{\mathbf{u}})^*) \cdot \mathbf{d}s \right) + c.c. \end{aligned} \quad (66)$$

By substituting Eq. (16) and Eq. (17) we have

$$\begin{aligned} P_{\text{piezo}} \approx & |b|^2 \left(\int (-\tilde{\mathbf{v}}^* \cdot (\mathbf{c} : \nabla \tilde{\mathbf{u}})) \cdot \mathbf{d}s \right) + b^* \left\{ \frac{\partial b}{\partial z} \left(\frac{M_{\text{RF}}^{(3)} - \frac{M_{\text{RF}}^{(1)} M_{\text{RF}}^{(4)}}{M_{\text{RF}}^{(2)}}}{M_{\text{RF}}^{(2)}} \right) + b \frac{M_{\text{RF}}^{(4)}}{M_{\text{RF}}^{(2)}} \right\} \\ & \left(\int (-\tilde{\mathbf{v}}^* \cdot (\mathbf{e} \cdot \nabla \tilde{\phi})) \cdot \mathbf{d}s \right) + \left| \left\{ \frac{\partial b}{\partial z} \left(\frac{M_{\text{RF}}^{(3)} - \frac{M_{\text{RF}}^{(1)} M_{\text{RF}}^{(4)}}{M_{\text{RF}}^{(2)}}}{M_{\text{RF}}^{(2)}} \right) + b \frac{M_{\text{RF}}^{(4)}}{M_{\text{RF}}^{(2)}} \right\} \right|^2 \\ & \left(\int \left(-i\Omega \tilde{\phi} ((\epsilon \cdot \nabla \tilde{\phi})^*) \cdot \mathbf{d}s \right) + \left\{ \frac{\partial b}{\partial z} \left(\frac{M_{\text{RF}}^{(3)} - \frac{M_{\text{RF}}^{(1)} M_{\text{RF}}^{(4)}}{M_{\text{RF}}^{(2)}}}{M_{\text{RF}}^{(2)}} \right) + b \frac{M_{\text{RF}}^{(4)}}{M_{\text{RF}}^{(2)}} \right\} b^* \left(\int (-i\Omega \tilde{\phi} (\mathbf{r} : \nabla \tilde{\mathbf{u}})^*) \cdot \mathbf{d}s \right) + c.c.. \end{aligned} \quad (67)$$

Here, by neglecting the differential terms, the power can be simplified as follows. This approximation is valid

as long as b has a slowly varying envelop and Ψ is equal to $\frac{M_{\text{RF}}^{(4)}}{M_{\text{RF}}^{(2)}} b$ according to Eq. (17).

$$P_{\text{piezo}} \approx |b|^2 (\mathcal{P}_{\text{pure}}^{\text{M}} + \mathcal{P}^{\text{MEL}} + \mathcal{P}_{\text{pure}}^{\text{El}} + \mathcal{P}^{\text{ELM}}) = |b|^2 (\mathcal{P}_{\text{tot}}^{\text{M}} + \mathcal{P}_{\text{tot}}^{\text{El}}) = |b|^2 \mathcal{P}_{\text{piezo}}, \quad (68)$$

where $\mathcal{P}_{\text{tot}}^{\text{M}}$ is acoustic power in a non-centrosymmetric

material and can be expressed by

$$\begin{aligned}
\mathcal{P}_{\text{tot}}^{\text{M}} &= -i\Omega \int \tilde{\mathbf{u}}^* \cdot \left((\mathbf{c} : \nabla \tilde{\mathbf{u}} + \frac{M_{\text{RF}}^{(4)}}{M_{\text{RF}}^{(2)}} (\mathbf{e} \cdot \nabla \tilde{\phi})) \right) \cdot \mathbf{d}\mathbf{s} + c.c. \\
&= \mathcal{P}_{\text{pure}}^{\text{M}} + \mathcal{P}^{\text{MEI}},
\end{aligned} \tag{69}$$

where $\mathcal{P}_{\text{pure}}^{\text{M}}$ and \mathcal{P}^{MEI} are pure mechanical power and mechanoelectrical power, respectively. It must be noted that pure mechanical power $\mathcal{P}_{\text{pure}}^{\text{M}}$ is the same with \mathcal{P}_{ac} ($\mathcal{P}_{\text{pure}}^{\text{M}} = \mathcal{P}_{\text{ac}}$). And they can be written as follows:

$$\begin{aligned}
\mathcal{P}_{\text{pure}}^{\text{M}} &= -i\Omega \int \tilde{\mathbf{u}}^* \cdot (\mathbf{c} : \nabla \tilde{\mathbf{u}}) \cdot \mathbf{d}\mathbf{s} + c.c., \\
\mathcal{P}^{\text{MEI}} &= -i\Omega \frac{M_{\text{RF}}^{(4)}}{M_{\text{RF}}^{(2)}} \int \tilde{\mathbf{u}}^* \cdot (\mathbf{e} \cdot \nabla \tilde{\phi}) \cdot \mathbf{d}\mathbf{s} + c.c.,
\end{aligned} \tag{70}$$

and $\mathcal{P}_{\text{tot}}^{\text{El}}$ is the total electrical part of the Poynting power in a piezoelectric medium, which can itself be divided to pure electrical and electromechanical power.

$$\begin{aligned}
\mathcal{P}_{\text{tot}}^{\text{El}} &= -i\Omega \left| \frac{M_{\text{RF}}^{(4)}}{M_{\text{RF}}^{(2)}} \right|^2 \int \tilde{\phi} (\epsilon \cdot \nabla \tilde{\phi})^* \cdot \mathbf{d}\mathbf{s} \\
&\quad - \frac{M_{\text{RF}}^{(4)}}{M_{\text{RF}}^{(2)}} i\Omega \int \tilde{\phi} (\mathbf{r} : \nabla \tilde{\mathbf{u}})^* \cdot \mathbf{d}\mathbf{s} + c.c. = \mathcal{P}_{\text{pure}}^{\text{El}} + \mathcal{P}^{\text{ElM}},
\end{aligned} \tag{71}$$

where

$$\begin{aligned}
\mathcal{P}_{\text{pure}}^{\text{El}} &= -i\Omega \left| \frac{M_{\text{RF}}^{(4)}}{M_{\text{RF}}^{(2)}} \right|^2 \int \tilde{\phi} (\epsilon \cdot \nabla \tilde{\phi})^* \cdot \mathbf{d}\mathbf{s} + c.c., \\
\mathcal{P}^{\text{ElM}} &= -i\Omega \frac{M_{\text{RF}}^{(4)}}{M_{\text{RF}}^{(2)}} \int \tilde{\phi} (\mathbf{r} : \nabla \tilde{\mathbf{u}})^* \cdot \mathbf{d}\mathbf{s} + c.c..
\end{aligned} \tag{72}$$

It should be noted that for many piezoelectric materials such as GaAs or AlN, the relation $M_{\text{RF}}^{(1)} = \left| \frac{M_{\text{RF}}^{(2)}}{M_{\text{RF}}^{(4)}} \right|^2 \mathcal{P}_{\text{pure}}^{\text{El}}$ occurs due to their isotropic material properties (i.e. having diagonal permittivity tensor (ϵ)). Also, for Bulky cubic crystal structure the electromechanical power is equal to absolute value of the mechanoelectrical power because the tensor of $\mathbf{e}_{ijk} = \mathbf{e}_{kij}$ [29], however; in an integrated the mode profile can play an important role. Therefore, in nano waveguide structure even with cubic crystal material the electromechanical power is not the same absolute value with the mechanoelectrical power.

C. Calculation of $A_{\text{p}}^* A_{\text{s}} \frac{\partial \Psi}{\partial z}$ and $A_{\text{p}}^* A_{\text{s}} \Psi$ Terms

By making an extra spacial derivative -along the propagation direction - of the acoustic envelope Eq. (37) and neglecting the second order derivative of the envelope (i.e. $\frac{\partial^2 \Psi}{\partial z^2} \approx \frac{\partial^2 b}{\partial z^2} \approx 0$), we reach the following relation

$$\frac{\partial b}{\partial z} = \gamma_1 \frac{\partial (A_{\text{p}} A_{\text{s}}^*)}{\partial z} + \gamma_2 \frac{\partial^2 \Psi}{\partial z^2} + \gamma_3 \frac{\partial \Psi}{\partial z} \approx \gamma_1 \frac{\partial (A_{\text{p}} A_{\text{s}}^*)}{\partial z} + \gamma_3 \frac{\partial \Psi}{\partial z}, \tag{73}$$

where γ_i (i=1,2,3)

$$\begin{aligned}
\gamma_1 &= \frac{-i\Omega \tilde{Q}_{\text{b}}}{\left(\alpha_{\text{ac}} - \frac{M_{\text{RF}}^{(4)}}{M_{\text{RF}}^{(3)}} \right) \mathcal{P}_{\text{ac}}}, \\
\gamma_2 &= \left(\frac{-i\Omega \tilde{Q}_{1,\text{piezo}}}{\left(\alpha_{\text{ac}} - \frac{M_{\text{RF}}^{(4)}}{M_{\text{RF}}^{(3)}} \right) \mathcal{P}_{\text{ac}}} - \frac{M_{\text{RF}}^{(1)}}{M_{\text{RF}}^{(3)} \left(\alpha_{\text{ac}} - \frac{M_{\text{RF}}^{(4)}}{M_{\text{RF}}^{(3)}} \right)} \right), \\
\gamma_3 &= \left(\frac{-i\Omega \tilde{Q}_{2,\text{piezo}}}{\left(\alpha_{\text{ac}} - \frac{M_{\text{RF}}^{(4)}}{M_{\text{RF}}^{(3)}} \right) \mathcal{P}_{\text{ac}}} - \frac{M_{\text{RF}}^{(2)}}{M_{\text{RF}}^{(3)} \left(\alpha_{\text{ac}} - \frac{M_{\text{RF}}^{(4)}}{M_{\text{RF}}^{(3)}} \right)} \right).
\end{aligned} \tag{74}$$

By substituting Eq. (16) in Eq. (73) and after a rearrangement and then by substituting Eq. (40) for the pump and Stokes derivatives and by knowing that $P_i = (-1)^\xi \mathcal{P}_i |A_i|^2$, the differential acoustic envelope variation in a relation with pump and Stokes envelope is expressed by

$$\begin{aligned}
\frac{\partial b}{\partial z} &\approx \left(\frac{\gamma_1}{1 - \gamma_3 \frac{M_{\text{RF}}^{(4)}}{M_{\text{RF}}^{(2)}}} \right) \frac{\partial(A_{\text{p}}A_{\text{s}}^*)}{\partial z} = \left(\frac{\gamma_1}{1 - \gamma_3 \frac{M_{\text{RF}}^{(4)}}{M_{\text{RF}}^{(2)}}} \right) A_{\text{s}}^* \frac{\partial A_{\text{p}}}{\partial z} + \frac{\gamma_1}{1 - \gamma_3 \frac{M_{\text{RF}}^{(4)}}{M_{\text{RF}}^{(2)}}} A_{\text{p}} \frac{\partial A_{\text{s}}^*}{\partial z} \\
&= \left(\frac{\gamma_1}{1 - \gamma_3 \frac{M_{\text{RF}}^{(4)}}{M_{\text{RF}}^{(2)}}} \right) \left(\frac{-i\omega_{\text{p}} \tilde{Q}_{\text{p}}}{\mathcal{P}_{\text{p}}} \right) |A_{\text{s}}|^2 b + \left(\frac{\gamma_1}{1 - \gamma_3 \frac{M_{\text{RF}}^{(4)}}{M_{\text{RF}}^{(2)}}} \right) \left(\frac{i\omega_{\text{s}} \tilde{Q}_{\text{s}}^*}{\mathcal{P}_{\text{s}}} \right) |A_{\text{p}}|^2 b \approx \gamma_4 (P_{\text{p}} - P_{\text{s}}) b,
\end{aligned} \tag{75}$$

where γ_4 is

$$\gamma_4 = \left(\frac{\gamma_1}{1 - \gamma_3 \frac{M_{\text{RF}}^{(4)}}{M_{\text{RF}}^{(2)}}} \right) \left(\frac{i\omega_{\text{p}} \tilde{Q}_{\text{p}}}{\mathcal{P}_{\text{p}} \mathcal{P}_{\text{s}}} \right). \tag{76}$$

Therefore, $\frac{\partial \Psi}{\partial z}$ can be calculated by $\frac{M_{\text{RF}}^{(4)}}{M_{\text{RF}}^{(2)}} \frac{\partial b}{\partial z}$ ($\frac{\partial \Psi}{\partial z} \approx \frac{M_{\text{RF}}^{(4)}}{M_{\text{RF}}^{(2)}} \frac{\partial b}{\partial z}$). And after replacing Eq. (75) in Eq. (17), equation of Ψ can be expressed as follows

$$\Psi \approx \left(\gamma_4 \left(\frac{M_{\text{RF}}^{(3)} - \frac{M_{\text{RF}}^{(1)} M_{\text{RF}}^{(4)}}{M_{\text{RF}}^{(2)}}}{M_{\text{RF}}^{(2)}} \right) \right) (P_{\text{p}} - P_{\text{s}}) b + \frac{M_{\text{RF}}^{(4)}}{M_{\text{RF}}^{(2)}} b. \tag{77}$$

Therefore, terms of Ψ and $\frac{\partial \Psi}{\partial z}$ are calculated based on pump, Stokes and acoustic envelopes. In continue, the

terms of $A_{\text{p}}A_{\text{s}}^*$ is realized. It is started with Eq. (37) and then by a substitution of Eq. (75) and Eq. (77), we have

$$\begin{aligned}
b &= \gamma_1 A_{\text{p}} A_{\text{s}}^* + \gamma_2 \frac{\partial \Psi}{\partial z} + \gamma_3 \Psi \\
&= \gamma_1 A_{\text{p}} A_{\text{s}}^* + \gamma_2 \gamma_4 \frac{M_{\text{RF}}^{(4)}}{M_{\text{RF}}^{(2)}} (P_{\text{p}} - P_{\text{s}}) b + \gamma_3 \gamma_4 \left(\frac{M_{\text{RF}}^{(3)} - \frac{M_{\text{RF}}^{(1)} M_{\text{RF}}^{(4)}}{M_{\text{RF}}^{(2)}}}{M_{\text{RF}}^{(2)}} \right) (P_{\text{p}} - P_{\text{s}}) b + \gamma_3 \frac{M_{\text{RF}}^{(4)}}{M_{\text{RF}}^{(2)}} b,
\end{aligned} \tag{78}$$

by a rearrangement, it is

$$A_{\text{p}} A_{\text{s}}^* = \left(\frac{1}{\gamma_1} - \frac{\gamma_3}{\gamma_1} \frac{M_{\text{RF}}^{(4)}}{M_{\text{RF}}^{(2)}} \right) b - \left(\frac{\gamma_2 \gamma_4}{\gamma_1} \frac{M_{\text{RF}}^{(4)}}{M_{\text{RF}}^{(2)}} + \frac{\gamma_3 \gamma_4}{\gamma_1} \left(\frac{M_{\text{RF}}^{(3)} - \frac{M_{\text{RF}}^{(1)} M_{\text{RF}}^{(4)}}{M_{\text{RF}}^{(2)}}}{M_{\text{RF}}^{(2)}} \right) \right) (P_{\text{p}} - P_{\text{s}}) b, \tag{79}$$

and then, we have

$$\begin{aligned}
A_{\text{p}}^* A_{\text{s}} \Psi &\approx \left(\left(\frac{1}{\gamma_1} - \frac{\gamma_3}{\gamma_1} \frac{M_{\text{RF}}^{(4)}}{M_{\text{RF}}^{(2)}} \right) b - \left(\frac{\gamma_2 \gamma_4}{\gamma_1} \frac{M_{\text{RF}}^{(4)}}{M_{\text{RF}}^{(2)}} + \frac{\gamma_3 \gamma_4}{\gamma_1} \left(\frac{M_{\text{RF}}^{(3)} - \frac{M_{\text{RF}}^{(1)} M_{\text{RF}}^{(4)}}{M_{\text{RF}}^{(2)}}}{M_{\text{RF}}^{(2)}} \right) \right) (P_{\text{p}} - P_{\text{s}}) b \right)^* \\
&\left(\left(\gamma_4 \left(\frac{M_{\text{RF}}^{(3)} - \frac{M_{\text{RF}}^{(1)} M_{\text{RF}}^{(4)}}{M_{\text{RF}}^{(2)}}}{M_{\text{RF}}^{(2)}} \right) \right) (P_{\text{p}} - P_{\text{s}}) b + \frac{M_{\text{RF}}^{(4)}}{M_{\text{RF}}^{(2)}} b \right) \\
&= \sigma_1 P_{\text{piezo}} P_{\text{p}} - \sigma_1 P_{\text{piezo}} P_{\text{s}} + \sigma_2 P_{\text{piezo}} P_{\text{p}}^2 + \sigma_2 P_{\text{piezo}} P_{\text{s}}^2 - 2\sigma_2 P_{\text{piezo}} P_{\text{p}} P_{\text{s}} + \sigma_3 P_{\text{piezo}},
\end{aligned} \tag{80}$$

where σ_i are

$$\begin{aligned}
\sigma_1 &= \frac{1}{\mathcal{P}_{\text{piezo}}} \left(-\frac{M_{\text{RF}}^{(4)}}{M_{\text{RF}}^{(2)}} \left(\frac{\gamma_2 \gamma_4}{\gamma_1} \frac{M_{\text{RF}}^{(4)}}{M_{\text{RF}}^{(2)}} + \frac{\gamma_3 \gamma_4}{\gamma_1} \left(\frac{M_{\text{RF}}^{(3)} - \frac{M_{\text{RF}}^{(1)} M_{\text{RF}}^{(4)}}{M_{\text{RF}}^{(2)}}}{M_{\text{RF}}^{(2)}} \right) \right)^* + \left(\gamma_4 \left(\frac{M_{\text{RF}}^{(3)} - \frac{M_{\text{RF}}^{(1)} M_{\text{RF}}^{(4)}}{M_{\text{RF}}^{(2)}}}{M_{\text{RF}}^{(2)}} \right) \left(\frac{1}{\gamma_1} - \frac{\gamma_3}{\gamma_1} \frac{M_{\text{RF}}^{(4)}}{M_{\text{RF}}^{(2)}} \right)^* \right) \right), \\
\sigma_2 &= \frac{-1}{\mathcal{P}_{\text{piezo}}} \left(\frac{\gamma_2 \gamma_4}{\gamma_1} \frac{M_{\text{RF}}^{(4)}}{M_{\text{RF}}^{(2)}} + \frac{\gamma_3 \gamma_4}{\gamma_1} \left(\frac{M_{\text{RF}}^{(3)} - \frac{M_{\text{RF}}^{(1)} M_{\text{RF}}^{(4)}}{M_{\text{RF}}^{(2)}}}{M_{\text{RF}}^{(2)}} \right) \right)^* \left(\gamma_4 \left(\frac{M_{\text{RF}}^{(3)} - \frac{M_{\text{RF}}^{(1)} M_{\text{RF}}^{(4)}}{M_{\text{RF}}^{(2)}}}{M_{\text{RF}}^{(2)}} \right) \right), \\
\sigma_3 &= \frac{1}{\mathcal{P}_{\text{piezo}}} \frac{M_{\text{RF}}^{(4)}}{M_{\text{RF}}^{(2)}} \left(\frac{1}{\gamma_1} - \frac{\gamma_3}{\gamma_1} \frac{M_{\text{RF}}^{(4)}}{M_{\text{RF}}^{(2)}} \right)^*,
\end{aligned} \tag{81}$$

and the other term is

$$\begin{aligned}
A_p^* A_s \frac{\partial \Psi}{\partial z} &\approx \left(\left(\frac{1}{\gamma_1} - \frac{\gamma_3}{\gamma_1} \frac{M_{\text{RF}}^{(4)}}{M_{\text{RF}}^{(2)}} \right) b - \left(\frac{\gamma_2 \gamma_4}{\gamma_1} \frac{M_{\text{RF}}^{(4)}}{M_{\text{RF}}^{(2)}} + \frac{\gamma_3 \gamma_4}{\gamma_1} \left(\frac{M_{\text{RF}}^{(3)} - \frac{M_{\text{RF}}^{(1)} M_{\text{RF}}^{(4)}}{M_{\text{RF}}^{(2)}}}{M_{\text{RF}}^{(2)}} \right) \right) (P_p - P_s) b \right)^* \left(\gamma_4 \frac{M_{\text{RF}}^{(4)}}{M_{\text{RF}}^{(2)}} (P_p - P_s) b \right) \\
&= \tau_1 P_{\text{piezo}} P_p - \tau_1 P_{\text{piezo}} P_s + \tau_2 P_{\text{piezo}} P_p^2 + \tau_2 P_{\text{piezo}} P_s^2 - 2\tau_2 P_{\text{piezo}} P_p P_s,
\end{aligned} \tag{82}$$

where τ_i are

$$\begin{aligned}
\tau_1 &= \frac{1}{\mathcal{P}_{\text{piezo}}} \left(\frac{1}{\gamma_1} - \frac{\gamma_3}{\gamma_1} \frac{M_{\text{RF}}^{(4)}}{M_{\text{RF}}^{(2)}} \right)^* \left(\gamma_4 \frac{M_{\text{RF}}^{(4)}}{M_{\text{RF}}^{(2)}} \right), \\
\tau_2 &= \frac{1}{\mathcal{P}_{\text{piezo}}} \left(- \left(\frac{\gamma_2 \gamma_4}{\gamma_1} \frac{M_{\text{RF}}^{(4)}}{M_{\text{RF}}^{(2)}} + \frac{\gamma_3 \gamma_4}{\gamma_1} \left(\frac{M_{\text{RF}}^{(3)} - \frac{M_{\text{RF}}^{(1)} M_{\text{RF}}^{(4)}}{M_{\text{RF}}^{(2)}}}{M_{\text{RF}}^{(2)}} \right) \right) \right)^* \left(\gamma_4 \frac{M_{\text{RF}}^{(4)}}{M_{\text{RF}}^{(2)}} \right),
\end{aligned} \tag{83}$$

and finally we have:

$$\begin{aligned}
\frac{\partial P_p}{\partial z} &= 2\Re\left\{\frac{-\Omega\omega_p|\tilde{Q}_b|^2}{\left(\alpha_{ac} + \frac{M_{RF}^{(4)}}{M_{RF}^{(3)}}\right)\mathcal{P}_{ac}\mathcal{P}_p}\right\}\mathcal{P}_p|A_p|^2|A_s|^2 + 2\Re\left\{-\frac{i\omega_p\tilde{Q}_p}{\mathcal{P}_p}\left(\frac{-i\Omega\tilde{Q}_{1,piezo}}{\left(\alpha_{ac} - \frac{M_{RF}^{(4)}}{M_{RF}^{(3)}}\right)\mathcal{P}_{ac}} - \frac{M_{RF}^{(1)}}{M_{RF}^{(3)}\left(\alpha_{ac} - \frac{M_{RF}^{(4)}}{M_{RF}^{(3)}}\right)}\right)\mathcal{P}_pA_p^*A_s\frac{\partial\Psi}{\partial z}\right\} \\
&+ 2\Re\left\{-\frac{i\omega_p\tilde{Q}_p}{\mathcal{P}_p}\left(\frac{-i\Omega\tilde{Q}_{2,piezo}}{\left(\alpha_{ac} - \frac{M_{RF}^{(4)}}{M_{RF}^{(3)}}\right)\mathcal{P}_{ac}} - \frac{M_{RF}^{(2)}}{M_{RF}^{(3)}\left(\alpha_{ac} - \frac{M_{RF}^{(4)}}{M_{RF}^{(3)}}\right)}\right)\mathcal{P}_pA_p^*A_s\Psi\right\}, \\
\frac{\partial P_s}{\partial z} &= 2\Re\left\{\frac{\Omega\omega_s|\tilde{Q}_b|^2}{\left(\alpha_{ac} + \frac{M_{RF}^{(4)}}{M_{RF}^{(3)}}\right)\mathcal{P}_{ac}\mathcal{P}_s}\right\}\mathcal{P}_s|A_p|^2|A_s|^2 + 2\Re\left\{\left(-\frac{i\omega_p\tilde{Q}_s}{\mathcal{P}_p}\left(\frac{-i\Omega\tilde{Q}_{1,piezo}}{\left(\alpha_{ac} - \frac{M_{RF}^{(4)}}{M_{RF}^{(3)}}\right)\mathcal{P}_{ac}} - \frac{M_{RF}^{(1)}}{M_{RF}^{(3)}\left(\alpha_{ac} - \frac{M_{RF}^{(4)}}{M_{RF}^{(3)}}\right)}\right)\mathcal{P}_pA_p^*A_s\frac{\partial\Psi}{\partial z}\right)^*\right\} \\
&2\Re\left\{\left(-\frac{i\omega_p\tilde{Q}_s}{\mathcal{P}_p}\left(\frac{-i\Omega\tilde{Q}_{2,piezo}}{\left(\alpha_{ac} - \frac{M_{RF}^{(4)}}{M_{RF}^{(3)}}\right)\mathcal{P}_{ac}} - \frac{M_{RF}^{(2)}}{M_{RF}^{(3)}\left(\alpha_{ac} - \frac{M_{RF}^{(4)}}{M_{RF}^{(3)}}\right)}\right)\mathcal{P}_pA_p^*A_s\Psi\right)^*\right\}, \\
\frac{\partial P_{piezo}}{\partial z} &= \mathcal{P}_{piezo}\left(b\frac{\partial b^*}{\partial z} + b^*\frac{\partial b}{\partial z}\right) = 2\Re\left\{\mathcal{P}_{piezo}b\frac{\partial b^*}{\partial z}\right\} = 2\Re\{\gamma_4^*\}P_{piezo}(P_p - P_s).
\end{aligned} \tag{84}$$
